5
Nuclear Reactor Dynamics

An understanding of the time-dependent behavior of the neutron population in a nuclear reactor in response to either a planned change in the reactor conditions or to unplanned and abnormal conditions is of the utmost importance to the safe and reliable operation of nuclear reactors. We saw in Chapter 2 that the response of the prompt neutrons is very rapid indeed. However, unless the reactor is supercritical on prompt neutrons alone, the delayed emission of a small fraction of the fission neutrons can slow the increase in neutron population to the delayed neutron precursor decay time scale of seconds, providing time for corrective control measures to be taken. If a change in conditions makes a reactor supercritical on prompt neutrons alone, only intrinsic negative feedback mechanisms that automatically provide a compensating change in reactor conditions in response to an increase in the neutron population can prevent a runaway increase in neutron population (and fission power level). However, some of the intrinsic changes in reactor conditions in response to a change in power level may enhance the power excursion (positive feedback), and others may be negative but delayed sufficiently long that the compensatory reactivity feedback is out of phase with the actual condition of the neutron population in the reactor, leading to power-level instabilities. These reactor dynamics phenomena, the methods used for their analysis, and the experimental techniques for determining the basic kinetics parameters that govern them are discussed in this chapter.

5.1
Delayed Fission Neutrons

Neutrons Emitted in Fission Product Decay

The dynamics of a nuclear reactor or any other fission chain-reacting system under normal operation is determined primarily by the characteristics of the delayed emission of neutrons from the decay of fission products. The total yield of delayed neutrons per fission, ν_d, depends on the fissioning isotope and generally increases with the energy of the neutron causing fission. Although there are a relatively large number of fission products which subsequently decay via neutron emission, the

Nuclear Reactor Physics. Weston M. Stacey

ISBN: 978-3-527-40679-1

Table 5.1 Delayed Neutron Parameters

	Fast Neutrons		Thermal Neutrons	
Group	Decay Constant λ_i (s^{-1})	Relative Yield β_i/β	Decay Constant λ_i (s^{-1})	Relative Yield β_i/β
^{233}U		$\nu_d = 0.00731$ $\beta = 0.0026$		$\nu_d = 0.00667$ $\beta = 0.0026$
1	0.0125	0.096	0.0126	0.086
2	0.0360	0.208	0.0337	0.299
3	0.138	0.242	0.139	0.252
4	0.318	0.327	0.325	0.278
5	1.22	0.087	1.13	0.051
6	3.15	0.041	2.50	0.034
^{235}U		$\nu_d = 0.01673$ $\beta = 0.0064$		$\nu_d = 0.01668$ $\beta = 0.0067$
1	0.0127	0.038	0.0124	0.033
2	0.0317	0.213	0.0305	0.219
3	0.115	0.188	0.111	0.196
4	0.311	0.407	0.301	0.395
5	1.40	0.128	1.14	0.115
6	3.87	0.026	3.01	0.042
^{239}Pu		$\nu_d = 0.0063$ $\beta = 0.0020$		$\nu_d = 0.00645$ $\beta = 0.0022$
1	0.0129	0.038	0.0128	0.035
2	0.0311	0.280	0.0301	0.298
3	0.134	0.216	0.124	0.211
4	0.331	0.328	0.325	0.326
5	1.26	0.103	1.12	0.086
6	3.21	0.035	2.69	0.044
^{241}Pu		$\nu_d = 0.0152$		$\nu_d = 0.0157$ $\beta = 0.0054$
1	—	—	0.0128	0.010
2	—	—	0.0297	0.229
3	—	—	0.124	0.173
4	—	—	0.352	0.390
5	—	—	1.61	0.182
6	—	—	3.47	0.016
^{232}Th		$\nu_d = 0.0531$ $\beta = 0.0203$		
1	0.0124	0.034		
2	0.0334	0.150		
3	0.121	0.155		
4	0.321	0.446		
5	1.21	0.172		
6	3.29	0.043		

Table 5.1 (Continued)

Group	Fast Neutrons		Thermal Neutrons	
	Decay Constant λ_i (s^{-1})	Relative Yield β_i/β	Decay Constant λ_i (s^{-1})	Relative Yield β_i/β
^{238}U		$\nu_d = 0.0460$		
		$\beta = 0.0164$		
1	0.0132	0.013		
2	0.0321	0.137		
3	0.139	0.162		
4	0.358	0.388		
5	1.41	0.225		
6	4.02	0.075		
^{240}Pu		$\nu_d = 0.0090$		
		$\beta = 0.0029$		
1	0.0129	0.028		
2	0.0313	0.273		
3	0.135	0.192		
4	0.333	0.350		
5	1.36	0.128		
6	4.04	0.029		

observed composite emission characteristics can be well represented by defining six effective groups of delayed neutron precursor fission products. Each group can be characterized by a decay constant, λ_i, and a relative yield fraction, β_i/β. The fraction of the total fission neutrons that are delayed is $\beta = \nu_d/\nu$. The parameters of delayed neutrons emitted by fission product decay of several relevant isotopes are given in Table 5.1.

Effective Delayed Neutron Parameters for Composite Mixtures

The delayed neutrons emitted by the decay of fission products are generally less energetic (average energy about 0.5 MeV) than the prompt neutrons (average energy about 1 MeV) released directly in the fission event. Thus these delayed neutrons will slow down quicker than the prompt neutrons and experience less probability for absorption and leakage in the process (i.e., the delayed and prompt neutrons have a difference in their effectiveness in producing a subsequent fission event). Since the energy distribution of the delayed neutrons differs from group to group, the different groups of delayed neutrons will also have a different effectiveness. Furthermore, a nuclear reactor will, of course, contain a mixture of fissionable isotopes (e.g., a uranium-fueled reactor will initially contain ^{235}U and ^{238}U, and after operation for some time will also contain some admixture of ^{239}Pu, ^{240}Pu, and so on; see Chapter 6).

To deal with this situation, it is necessary to define an *importance function*, $\phi^+(r, E)$, which is the probability that a neutron introduced at position r and en-

ergy E will ultimately result in a fission (Chapter 13). Then the relative importance (to the production of a subsequent fission) of delayed neutrons in group i emitted with energy distribution $\chi_{di}^{q}(E)$ and prompt neutrons from the fission of isotope q emitted with energy distribution $\chi_{p}^{q}(E)$ are

$$I_{di}^{q} = \int dV \int_0^\infty dE\, \chi_{di}^{q}(E)\phi^{+}(r,E) \int_0^\infty dE'\, \nu\sigma_f^q(E')N_q(r)\phi(r,E') \tag{5.1}$$

$$I_{p}^{q} = \int dV \int_0^\infty dE\, \chi_{p}^{q}(E)\phi^{+}(r,E) \int_0^\infty dE'\, \nu\sigma_f^q(E')N_q(r)\phi(r,E') \tag{5.2}$$

The relative effective delayed neutron yield of group i delayed neutrons for fissionable isotope q is $I_{di}^{q}\beta_i^q$, where β_i^q is the group i delayed neutron yield of fissionable isotope q given in Table 5.1. The effective group i delayed neutron fraction for isotope q in a mixture of fissionable isotopes is then

$$\overline{\gamma_i\beta_i^q} = I_{di}^{q}\beta_i^q \Big/ \sum_q \left[I_{p}^{q}\left(1 - \sum_{i=1}^{6}\beta_i^q\right) + \sum_{i=1}^{6} I_{di}^{q}\beta_i^q \right] \tag{5.3}$$

The effectiveness of delayed neutron group i of fissionable isotope q in a specific admixture of fissionable isotopes and reactor geometry is then $\gamma_i^q = \overline{\gamma_i^q\beta_i^q}/\beta_i^q$. In the remainder of the book, except when specifically stated otherwise, it is assumed that the delayed neutron effectiveness is included in the evaluation of β_i and β, and the effectiveness parameter will be suppressed.

Photoneutrons

Fission products also emit gamma rays when they undergo β-decay. A photon can eject a neutron from a nucleus when its energy exceeds the neutron binding energy. Although most nuclei have neutron binding energies in excess of 6 MeV, which is above the energy of most gamma rays from fission, there are four nuclei that have sufficiently low neutron binding energy, E_n, to be of practical interest: ^{2}D ($E_n = 2.2$ MeV), ^{9}Be ($E_n = 1.7$ MeV), ^{6}Li ($E_n = 5.4$ MeV), and ^{13}C ($E_n = 4.9$ MeV). The photoneutrons can be considered as additional groups of delayed neutrons. Since the β-decay of fission products is generally much slower than the direct neutron decay, the photoneutron precursor decay constants are much smaller than the delayed neutron precursor decay constants shown in Table 5.1. The only reactors in which photoneutrons are of practical importance are D_2O-moderated reactors. As we shall see, the dynamic response time of a reactor under normal operation is largely determined by the inverse decay constants, and consequently, D_2O reactors are quite sluggish compared to other reactor types.

5.2
Point Kinetics Equations

The delayed neutron precursors satisfy an equation of the form

$$\frac{\partial \hat{C}_i}{\partial t}(r,t) = \beta_i \nu \Sigma_f(r,t)\phi(r,t) - \lambda_i \hat{C}_i(r,t), \quad i = 1,\ldots,6 \tag{5.4}$$

The one-speed neutron diffusion equation is now written

$$\begin{aligned}&\frac{1}{\mathrm{v}}\frac{\partial \phi(r,t)}{\partial t} - D(r,t)\nabla^2\phi(r,t) + \Sigma_a(r,t)\phi(r,t)\\ &\quad = (1-\beta)\nu\Sigma_F(r,t)\phi(r,t) + \sum_{i=1}^{6}\lambda_i \hat{C}_i(r,t)\end{aligned} \tag{5.5}$$

where we have taken into account that a fraction β of the fission neutrons is delayed and that there is a source of neutrons due to the decay of the delayed neutron precursors.

Based on the results of Chapter 3, we assume a separation-of-variables solution

$$\phi(r,t) = \mathrm{v}n(t)\psi_1(r), \qquad \hat{C}_i(r,t) = C_i(t)\psi_1(r) \tag{5.6}$$

where ψ_1 is the fundamental mode solution of

$$\nabla^2\psi_n + B_g^2\psi_n = 0 \tag{5.7}$$

and B_g is the geometric buckling appropriate for the reactor geometry, as discussed in Chapter 3. Using this in Eqs. (5.4) and (5.5) leads to the point kinetics equations

$$\begin{aligned}\frac{dn(t)}{dt} &= \frac{\rho(t)-\beta}{\Lambda}n(t) + \sum_{i=1}^{6}\lambda_i C_i(t)\\ \frac{dC_i(t)}{dt} &= \frac{\beta_i}{\Lambda}n(t) - \lambda_i C_i(t), \quad i = 1,\ldots,6\end{aligned} \tag{5.8}$$

where

$$\Lambda \equiv (\mathrm{v}\nu\Sigma_F)^{-1} \tag{5.9}$$

is the mean generation time between the birth of a fission neutron and the subsequent absorption leading to another fission, and

$$\rho(t) \equiv \frac{\nu\Sigma_F - \Sigma_a(1+L^2B_g^2)}{\nu\Sigma_F} \equiv \frac{k(t)-1}{k(t)} \tag{5.10}$$

is the reactivity. The quantity k is the effective multiplication constant, given by

$$k \equiv \frac{\nu\Sigma_F/\Sigma_a}{1+L^2B_g^2} \tag{5.11}$$

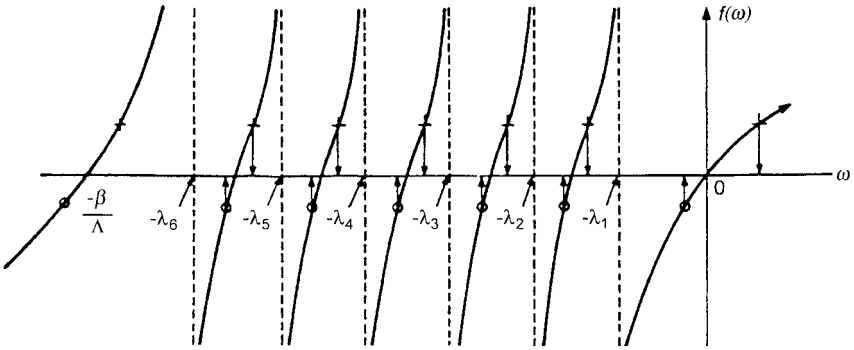

Fig. 5.1 Plot of the function $R(\omega) = \omega[\Lambda + \Sigma\beta_i/(\omega + \lambda_i)]$, which appears in the in-hour equation. (From Ref. 4; used with permission of MIT Press.)

For predominantly thermal reactors, $\nu\Sigma_f$ and Σ_a are thermal cross sections, and L^2 should be replaced by $M^2 = L^2 + \tau_{\text{th}}$ to include the fast diffusion while the neutron is slowing down, τ_{th}, as well as the thermal diffusion length, L^2. For fast reactors, all cross sections are averaged over the appropriate fast spectrum.

The limiting assumption for the validity of the point kinetics equations is the assumption of a constant spatial shape. As we will see, this assumption is reasonable for transients caused by uniform changes in reactor properties or for reactors with dimensions that are only a few migration lengths, M (or diffusion lengths, L), but is poor for reactors with dimensions that are very large compared to M in which the transient is caused by localized changes in reactor properties (e.g., a nonsymmetric control rod withdrawal). However, as we will see in Chapter 16, such spatial shape changes can be taken into account in computation of the reactivity and the mean generation time, and the point kinetics equations can be extended to have a much wider range of validity.

5.3 Period–Reactivity Relations

Equations (5.8) may be solved for the case of an initially critical reactor in which the properties are changed at $t = 0$ in such a way as to introduce a reactivity ρ_0 which is then constant over time, by Laplace transforming, or equivalently assuming an exponential time dependence e^{-st}. The equations for the time-dependent parts of n and C_i are

$$\begin{aligned} sn(s) &= \frac{\rho_0 - \beta}{\Lambda} n(s) + \sum_{i=1}^{6} \lambda_i C_i(s) + n_0 \\ sC_i(s) &= \frac{\beta_i}{\Lambda} n(s) - \lambda_i C_i(s) + C_{i0}, \quad i = 1, \ldots, 6 \end{aligned} \tag{5.12}$$

which can be reduced to

$$n(s) = \frac{f(s, n_0, C_{i0})}{Y(s)} \tag{5.13}$$

where

$$Y(s) \equiv \rho_0 - s\left(\Lambda + \sum_{i=1}^{6} \frac{\beta_i}{s + \lambda_i}\right) \tag{5.14}$$

The poles of the right side—the roots of $Y(s) = 0$—determine the time dependence of the neutron and precursor populations. $Y(s) = 0$ is a seventh-order equation, known as the *inverse hour*, or more succinctly, the *inhour*, equation, the solutions of which are best visualized graphically, as indicated in Fig. 5.1, where the right-hand side of

$$\rho_0 = s\left(\Lambda + \sum_{i=1}^{6} \frac{\beta_i}{s + \lambda_i}\right) \tag{5.15}$$

is plotted. The left-hand side, ρ_0, would plot as a straight horizontal line, of course, and the points at which it crosses the right-hand side are the solutions (roots of the equation). For $\rho_0 < 0$, indicated by the circles in Fig. 5.1, all the solutions $s_j < 0$. For $\rho_0 > 0$, indicated by the crosses, there are one positive and six negative solutions.

The solution for the time-dependent neutron flux is of the form

$$n(t) = \sum_{j=0}^{6} A_j e^{s_j t} \tag{5.16}$$

where the s_j are the roots of $Y(s) = 0$ and the A_j are given by

$$A_j = \left(\Lambda + \sum_{i=1}^{6} \frac{\beta_i}{s_j + \lambda_i}\right) \Bigg/ \left[1 + k \sum_{i=1}^{6} \frac{\beta_i \lambda_i}{(s_j + \lambda_i)^2}\right] \tag{5.17}$$

After a sufficient time, the solution will be dominated by the largest root s_0 ($s_0 > 0$ when $\rho_0 > 0$, s_0 is the least negative root when $\rho_0 < 0$):

$$n(t) \simeq A_0 e^{s_0 t} \equiv A_0 e^{t/T} \tag{5.18}$$

where $T \equiv s_0^{-1}$ is referred to as the *asymptotic period*. Measurement of the asymptotic period then provides a means for the experimental determination of the reactivity

$$\rho_0 = \frac{1}{T}\left[\Lambda + \sum_{i=1}^{6} \frac{\beta_i}{(1/T) + \lambda_i}\right] \tag{5.19}$$

5.4
Approximate Solutions of the Point Neutron Kinetics Equations

One Delayed Neutron Group Approximation

To simplify the problem so that we can gain insight into the nature of the solution of the point kinetics equations, we assume that the six groups of delayed neutrons can be replaced by one delayed neutron group with an effective yield fraction $\beta = \Sigma_i \gamma_i \beta_i$ and an effective decay constant $\lambda = \Sigma_i \beta_i \lambda_i / \beta$, so that the point kinetics equations become

$$\frac{dn}{dt} = \frac{\rho - \beta}{\Lambda} n + \lambda C, \qquad \frac{dC}{dt} = \frac{\beta}{\Lambda} n - \lambda C \tag{5.20}$$

Proceeding as in Section 5.3 by Laplace transforming or assuming an e^{st} form of the solution, the equivalent of Eq. (5.13) for the determination of the roots of the reduced in-hour equation is

$$s^2 - \left(\frac{\rho - \beta}{\Lambda} - \lambda \right) s - \frac{\lambda \rho}{\Lambda} = 0 \tag{5.21}$$

which has the solution

$$\begin{aligned} s_{1,2} &= \frac{1}{2}\left(\frac{\rho - \beta}{\Lambda} - \lambda \right) \pm \sqrt{\frac{1}{4}\left(\frac{\rho - \beta}{\Lambda} + \lambda \right)^2 + \frac{\beta \lambda}{\Lambda}} \\ &= \frac{1}{2}\left(\frac{\rho - \beta}{\Lambda} - \lambda \right) \pm \sqrt{\frac{1}{4}\left(\frac{\rho - \beta}{\Lambda} - \lambda \right)^2 + \frac{\lambda \rho}{\Lambda}} \end{aligned} \tag{5.22}$$

For $\rho > 0$, one root is positive and the other negative; for $\rho = 0$, one root is zero and the other is negative; and for $\rho < 0$, both roots are negative.

The assumed e^{st} time dependence, when used in Eqs. (5.20), requires that for each of the two roots, s_1 and s_2, there is a fixed relation between the precursor and the neutron populations:

$$\frac{C(t)}{n(t)} = \frac{\beta}{\Lambda(s_{1,2} + \lambda)} = -\left(\frac{\rho - \beta}{\Lambda} - s_{1,2} \right) \Big/ \lambda \tag{5.23}$$

which means that the solution of Eqs. (5.20) is of the form

$$n(t) = A_1 e^{s_1 t} + A_2 e^{s_2 t}, \qquad C(t) = A_1 \frac{\beta}{\Lambda(s_1 + \lambda)} e^{s_1 t} + A_2 \frac{\beta}{\Lambda(s_2 + \lambda)} e^{s_2 t} \tag{5.24}$$

Now, let us take some parameters typical of a light water reactor: $\beta = 0.0075$, $\lambda = 0.08\ \text{s}^{-1}$, $\Lambda = 6 \times 10^{-5}$ s. Except for $|\rho - \beta| \approx 0$, one root of Eq. (5.21) will be of very large magnitude, and the other will be of very small magnitude. For the larger root, $s_1^2 \gg \lambda \rho / \Lambda$ and $\lambda \rho / \Lambda$ can be neglected in Eq. (5.21); and for the

smaller root, $s_2^2 \ll \lambda\rho/\Lambda$ and s_2^2 can be neglected. Assuming that $|\rho - \beta|/\Lambda \gg \lambda$, the solutions of Eq. (5.21) are

$$s_1 = \frac{\rho - \beta}{\Lambda}, \qquad s_2 = -\frac{\lambda\rho}{\rho - \beta} \tag{5.25}$$

The constants A_1 and A_2 can be evaluated by requiring that the solution satisfy the initial condition at $t = 0$ that is determined by setting $\rho = 0$ in Eqs. (5.24), which identifies $A_1 \approx n_0\rho/(\rho - \beta)$ and $A_2 \approx -n_0\beta/(\rho - \beta)$, where n_0 is the initial neutron population before the reactivity insertion, so that the solutions of Eqs. (5.24) become

$$\begin{aligned} n(t) &= n_0\left[\frac{\rho}{\rho - \beta}\exp\left(\frac{\rho - \beta}{\Lambda}t\right) - \frac{\beta}{\rho - \beta}\exp\left(-\frac{\lambda\rho}{\rho - \beta}t\right)\right] \\ c(t) &= n_0\left[\frac{\rho\beta}{(\rho - \beta)^2}\exp\left(\frac{\rho - \beta}{\Lambda}t\right) + \frac{\beta}{\Lambda\lambda}\exp\left(-\frac{\lambda\rho}{\rho - \beta}t\right)\right] \end{aligned} \tag{5.26}$$

At $t = 0$, before the reactivity insertion, $C_0 = \beta n_0/\Lambda\lambda \approx 1600 n_0$. Thus the population of delayed neutron precursors, hence the latent source of neutrons, is about 1600 times greater than the neutron population in a critical reactor. It is not surprising that this large latent neutron source controls the dynamics of the neutron population under normal conditions, as we shall now see.

Example 5.1: Step Negative Reactivity Insertion, $\rho < 0$. Equations (5.26) enable us to investigate the neutron kinetics of a nuclear reactor. We first consider the case of a large negative reactivity insertion $\rho = -0.05$ into a critical reactor at $t = 0$, such as might be produced by scramming (rapid insertion) of a control rod bank. With the representative light water reactor parameters ($\beta = 0.0075$, $\lambda = 0.08\ \text{s}^{-1}$, $\Lambda = 6 \times 10^{-5}$ s), Eqs. (5.26) become

$$\begin{aligned} n(t) &= n_0(0.87e^{-958t} + 0.13e^{-0.068t}) \\ C(t) &= n_0(0.0113e^{-958t} + 1563e^{-0.068t}) \end{aligned} \tag{5.27}$$

which is plotted in Fig. 5.2, with $T \equiv n$. The first term goes promptly to zero on a time scale $\Delta t \approx \Lambda$, corresponding physically to readjustment of the prompt neutron population to the subcritical condition of the reactor on the neutron generation time scale. The second term decays slowly, corresponding to the slow decay of the delayed neutron precursor source of neutrons. The neutron population drops promptly from n_0 to $n_0/(1 - \rho/\beta)$—the *prompt jump*—then slowly decays as $e^{-[\lambda/(1-\beta/\rho)]t}$. Thus, scramming a control rod bank cannot immediately shut down (reduce the neutron population or the fission rate to near zero) a nuclear reactor or other fission chain reacting medium. The delayed neutron precursors decay as $e^{-[\lambda/(1-\beta/\rho)]t}$.

Example 5.2: Subprompt-Critical (Delayed Critical) Step Positive Reactivity Insertion, $0 < \rho < \beta$. Next, consider a positive reactivity insertion $\rho = 0.0015 < \beta$, such as

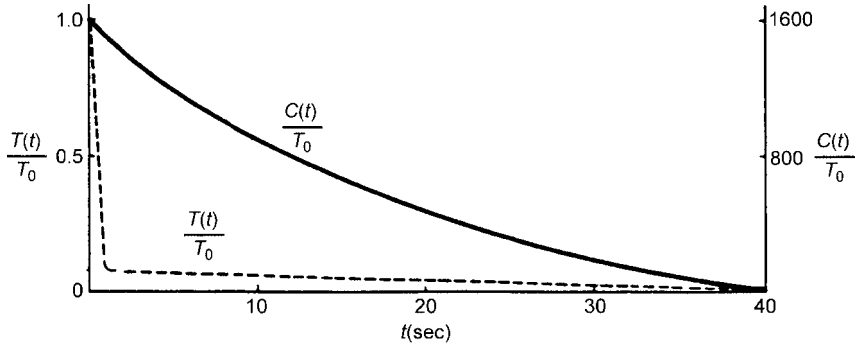

Fig. 5.2 Neutron and delayed neutron precursor decay following negative reactivity insertion $\rho = -0.05$ into a critical nuclear reactor. (From Ref. 4; used with permission of MIT Press.)

might occur as a result of control rod withdrawal. Equations (5.26) now become

$$\begin{aligned} n(t) &= n_0(-0.25e^{-100t} + 1.25e^{0.02t}) \\ C(t) &= n_0(0.3125e^{-100t} + 1562.5e^{0.02t}) \end{aligned} \tag{5.28}$$

which is plotted in Fig. 5.3. The neutron population increases promptly, on the neutron generation time scale—the prompt jump—from n_0 to $n_0/(1 - \rho/\beta)$, as the prompt neutron population adjusts to the supercritical condition of the reactor, then increases as $e^{-[\lambda/(1-\beta/\rho)]t}$, governed by the rate of increase in the delayed neutron source. The relatively slow rate of increase of the neutron population, following the prompt jump, allows time for corrective control action to be taken before the fission rate becomes excessive.

Example 5.3: Superprompt-Critical Step Positive Reactivity Insertion, $\rho > \beta$. Now consider a step increase of reactivity $\rho = 0.0115 > \beta$, such as might occur as the result

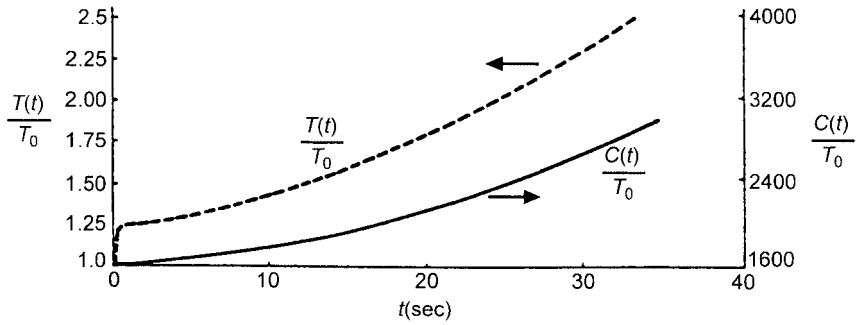

Fig. 5.3 Neutron and delayed neutron precursor increase following subprompt-critical positive reactivity insertion $\rho = 0.0015 < \beta$ into a critical nuclear reactor. (From Ref. 4; used with permission of MIT Press.)

of the ejection of a bank of control rods from a reactor. Equations (5.26) now become

$$\begin{aligned} n(t) &= n_0(2.9e^{66.7t} - 1.9e^{-0.23t}) \\ C(t) &= n_0(5.4e^{66.7t} + 1563e^{-0.23t}) \end{aligned} \tag{5.29}$$

The neutron population in the reactor grows exponentially on the neutron generation time scale, $n \sim e^{[(\rho-\beta)/\Lambda]t}$, because the reactor is supercritical on prompt neutrons alone [i.e., $k(1-\beta) > 1$]. In this example, the neutron population would increase by almost a factor of 800 in a tenth of a second, and it would be impossible to take corrective action quickly enough to prevent excessive fission heating and destruction of the reactor. Fortunately, there are inherent feedback mechanisms that introduce negative reactivity instantaneously in response to an increase in the fission heating (e.g., the Doppler effect discussed in Sections 5.7 and 5.8), and the neutron population will first increase rapidly, then decrease. However, conditions that would lead to superprompt-critical reactivity insertion are to be avoided for reasons of safety. Since $\beta = 0.0026$ for ^{233}U, 0.0067 for ^{235}U, and 0.0022 ^{239}Pu, the safe operating range for positive reactivity insertions, $0 < \rho < \beta$, is much larger for reactors fueled with ^{235}U than for reactors fueled with ^{233}U or ^{239}Pu.

Prompt-Jump Approximation

We found that with a reactivity insertion for which the reactor condition is less than prompt critical ($\rho < \beta$) the neutron population changed sharply on the neutron generation time scale, then changed slowly on the delayed neutron inverse decay constant time scale. If we are not interested in the details of the prompt neutron kinetics during the prompt jump, we can simplify the equations by assuming that the prompt jump takes place instantaneously in response to any reactivity change, and afterward, the neutron population changes instantaneously in response to changes in the delayed neutron source (i.e., we set the time derivative to zero in the neutron equation).

$$0 = [\rho(t) - \beta]n(t) + \Lambda \sum_{i=1}^{6} \lambda_i C_i(t) \tag{5.30}$$

Since the delayed neutron precursor population does not respond instantaneously to a change in reactivity, Eq. (5.30) is valid with the same delayed precursor population both before and just after a change in reactivity from ρ_0 to $\rho_1 < \beta$, from which we conclude that the ratio of the neutron populations just after and before the reactivity change is

$$\frac{n_1}{n_0} = \frac{\beta - \rho_0}{\beta - \rho_1} \tag{5.31}$$

Use of Eq. (5.30) to eliminate $n(t)$ in the second of Eqs. (5.8) yields a coupled set of equations for the time dependence of the precursor density:

$$\frac{dC_i}{dt} = \frac{\beta_i}{\rho(t) - \beta_i} \sum_{j=1}^{6} \lambda_j C_j(t) - \lambda_i C_i(t) \tag{5.32}$$

which in the one delayed precursor group approximation takes on the simple form

$$\frac{dC(t)}{dt} = \frac{-\lambda C(t)}{1 - \beta/\rho(t)} \tag{5.33}$$

The prompt-jump approximation is convenient for numerical solutions because it eliminates the fast time scale due to Λ, which introduces difficulties in time differencing methods. Numerical solutions of the point kinetics equations with and without the prompt-jump approximation for a variety of reactivity insertions indicate that the prompt-jump approximation is accurate to within about 1% for reactivities $\rho < 0.5\beta$.

Using the one delayed precursor group approximation, the equivalent of Eq. (5.30) can be solved for $C(t)$ and used in the second of Eqs. (5.20) to obtain

$$[\rho(t) - \beta]\frac{dn(t)}{dt} + \left[\frac{d\rho(t)}{dt} + \lambda\rho(t)\right]n(t) = 0 \tag{5.34}$$

which for a given reactivity variation $\rho(t)$ can be solved for the neutron population

$$n(t) = n_0 \exp\left[\int_0^t \frac{\dot{\rho}(t') + \lambda\rho(t')}{\beta - \rho(t')}\, dt'\right] \tag{5.35}$$

Example 5.4: Reactivity Worth of Rod Insertion. The neutron flux measured by a detector is observed to drop instantaneously from n_0 to 0.5 n_0 when a control rod is dropped into a cold highly enriched critical nuclear reactor, in which $\rho_0 = 0$. Using the one-delayed group model with $\beta = 0.0065$, Eq. (5.31) yields $\rho_1 = \beta(1 - n_0/n_1) = 0.0065(1 - 2) = -0.0065\Delta k/k$.

Reactor Shutdown

We mentioned that the large step negative reactivity insertion considered previously might be representative of the situation encountered in a reactor shutdown, or scram. However, the time required to fully insert control rods is very long compared to the prompt neutron generation time that governs the time scale of the prompt jump. We can improve on the representation of the control rod insertion by considering a ramp reactivity insertion $\rho(t) = -\varepsilon t$. If we are only interested in calculating the initial rapid decrease in the neutron population, we can make the assumption that the initial precursor concentration remains constant; hence the precursor source of delayed neutrons remains constant at its pre-insertion value

$$\sum_{i=1}^{6} \lambda_i C_i(0) = \frac{\beta}{\Lambda} n_0 \tag{5.36}$$

Using this approximation, the equation governing the prompt neutron response to the reactivity insertion—the first of Eqs. (5.8)—can be integrated to obtain

$$n(t) = n_0\left[\exp\left[-\frac{1}{\Lambda}\left(\frac{1}{2}\varepsilon t^2 + \beta t\right)\right] + \frac{\beta}{\Lambda}\int_0^t \exp\left\{-\frac{1}{\Lambda}\left[\frac{\varepsilon}{2}(t^2 - (t')^2) + \beta(t - t')\right]\right\} dt'\right] \tag{5.37}$$

This provides a somewhat better description of the initial reduction in the neutron population than do Eqs. (5.27), which, however, would still govern the long-time decay after completion of the rod insertion.

5.5
Delayed Neutron Kernel and Zero-Power Transfer Function

Delayed Neutron Kernel

The delayed neutron precursor equations, the second of Eqs. (5.8), can be formally integrated to obtain (assuming that $C_i = 0$ at $-\infty$)

$$C_i(t) = \int_{-\infty}^{t} \frac{\beta_i}{\Lambda} n(t') e^{-\lambda_i (t - t')}\, dt' = \int_0^{\infty} \frac{\beta_i}{\Lambda} e^{-\lambda_i \tau} n(t - \tau)\, d\tau. \tag{5.38}$$

Using this result in the neutron kinetics equation, the first of Eqs. (5.8), yields

$$\frac{dn(t)}{dt} = \left(\frac{\rho(t) - \beta}{\Lambda}\right) n(t) + \int_0^{\infty} \frac{\beta}{\Lambda} D(\tau) n(t - \tau)\, d\tau \tag{5.39}$$

where we have defined the delayed neutron kernel

$$D(\tau) \equiv \sum_{i=1}^{6} \frac{\lambda_i \beta_i}{\beta} e^{-\lambda_i \tau} \tag{5.40}$$

Zero-Power Transfer Function

If the neutron population is expanded about the initial neutron population in the critical reactor at $t = 0$,

$$n(t) = n_0 + n_1(t) \tag{5.41}$$

Eq. (5.39) may be rewritten

$$\frac{dn_1(t)}{dt} = \frac{\rho(t) n_0}{\Lambda} + \frac{\rho(t) n_1(t)}{\Lambda} + \int_0^{\infty} \frac{\beta}{\Lambda} D(\tau)[n_1(t - \tau) - n_1(t)]\, d\tau \tag{5.42}$$

The Laplace transform of a function of time $A(t)$ is defined as

$$A(s) = \int_0^{\infty} A(t) e^{-st}\, dt \tag{5.43}$$

Laplace transforming Eq. (5.42) and using the convolution theorem

$$\mathcal{L}\left[\int_0^\infty A(t)B(\tau - t)\,dt\right] = A(s)B(s) \tag{5.44}$$

yields, upon assuming that the term $\rho(t)n_1(t)$ is a product of two small terms and can be neglected relative to $\rho(t)n_0$,

$$n_1(s) = n_0 Z(s)\rho(s) \tag{5.45}$$

where

$$Z(s) \equiv \frac{1}{s}\left(\Lambda + \sum_{i=1}^{6} \frac{\beta_i}{s + \lambda_i}\right)^{-1} \tag{5.46}$$

is the *zero-power transfer function*, which defines the response of the density n_1 to the reactivity.

The inverse Laplace transformation of Eq. (5.45) and the convolution theorem yield the solution for the time dependence of the neutron population as a function of the time dependence of the reactivity:

$$n_1(t) = n_0 \int_0^t d\tau\, Z(t - \tau)\rho(\tau) \tag{5.47}$$

where the inverse Laplace transform of the zero-power transfer function is

$$Z(t - \tau) = \frac{1}{\Lambda} + \sum_{j=2}^{7} \frac{e^{s_j(t-\tau)}}{s_j\{\Lambda + \sum_{i=1}^{6}[\beta_i\lambda_i/(s_j + \lambda_i)^2]\}} \tag{5.48}$$

and the s_j are the roots of the inhour equation, $Y(s) = 0$, with $Y(s)$ given by Eq. (5.14).

5.6
Experimental Determination of Neutron Kinetics Parameters

Asymptotic Period Measurement

When a critical reactor is perturbed by a step change in properties, the asymptotic period may be determined from the response $R(t)$ of neutron detectors by $T^{-1} = d(\ln R)/dt$; then the period–reactivity relation of Eq. (5.19) can be used to infer the reactivity. For negative reactivities, the asymptotic period, the largest root of the inhour equation, is dominated by the largest delayed neutron period and is relatively insensitive to the value of the reactivity, so this method is limited practically to supercritical reactivity ($0 < \rho$) measurements, for which Eq. (5.19) may be written

$$\frac{\rho}{\beta} = \frac{\Lambda}{\beta T} + \sum_{i=1}^{6} \frac{\beta_i/\beta}{1 + \lambda_i T} \simeq \sum_{i=1}^{6} \frac{\beta_i/\beta}{1 + \lambda_i T} \tag{5.49}$$

where the fact that safety considerations further limit the practical applicability of this method to the delayed critical regime ($0 < \rho < \beta$) has been taken into account in writing the second form of the equation.

Rod Drop Method

The responses of a neutron detector immediately before ($R_0 \sim n_0$) and after ($R_1 \sim n_1$) a control rod is dropped into a critical reactor ($\rho_0 = 0$) are related by Eq. (5.31), which allows determination of the reactivity worth of the rod

$$\frac{\rho_1}{\beta} = 1 - \frac{R_0}{R_1} \tag{5.50}$$

Source Jerk Method

Consider a subcritical system that is maintained at equilibrium neutron, n_0, and precursor, C_{i0}, populations by an extraneous neutron source rate, S. The neutron balance equation is

$$\left(\frac{\rho - \beta}{\Lambda}\right) n_0 + \sum_{i=1}^{6} \lambda_i C_{i0} + S = 0 \tag{5.51}$$

If the source is jerked, the prompt-jump approximation for the neutron density immediately after the source jerk is

$$\left(\frac{\rho - \beta}{\Lambda}\right) n_1 + \sum_{i=1}^{6} \lambda_i C_{i0} = 0 \tag{5.52}$$

because the delayed neutron precursor population will not change immediately. These equations and the equilibrium precursor concentrations $C_{i0} = \beta_i n_0 / \lambda_i \Lambda$ may be used to relate the responses of a neutron detector immediately before ($R_0 \sim n_0$) and after ($R_1 \sim n_1$) the source jerk to the reactivity of the system:

$$\frac{\rho}{\beta} = 1 - \frac{R_0}{R_1} \tag{5.53}$$

Pulsed Neutron Methods

The time dependence of the prompt neutron population in a subcritical fission chain reacting medium following the introduction of a burst of neutrons is described by

$$\frac{1}{\mathrm{v}} \frac{\partial \phi(r,t)}{\partial t} = D\nabla^2 \phi(r,t) - [\Sigma_a - (1-\beta)\nu\Sigma_f]\phi(r,t) \tag{5.54}$$

since the delayed neutrons will not contribute until later. As discussed in Section 3.6, the asymptotic solution that remains after higher-order spatial transients decay is the fundamental mode, which decays exponentially:

$$n(r,t) \simeq A_1 \psi_1(r) e^{-\mathrm{v}[\Sigma_a - (1-\beta)\nu\Sigma_f + DB_g^2]t} \tag{5.55}$$

where B_g is the fundamental mode geometric buckling for the geometry of the system.

If the neutron detector response, $R(\mathbf{r}, t) \sim n(\mathbf{r}, t)$, is measured as a function of time, then

$$\alpha_0 = \frac{1}{R}\frac{dR}{dt} = \mathrm{v}\left[\nu\Sigma_f(1-\beta) - \Sigma_a - DB_g^2\right] = \frac{\rho-\beta}{\Lambda} \tag{5.56}$$

Thus the pulsed neutron method can be used to determine $\sim \rho/\Lambda$, assuming that β/Λ is known. If the experiment is performed in a critical system ($\rho = 0$), the measurement yields a value for β/Λ. In practice, a correction must be made to account for transport- and energy-dependent effects which have been neglected in this analysis, so that

$$\alpha_0 = \mathrm{v}\left[\nu\Sigma_f(1-\beta) - \Sigma_a - DB_g^2 - CB_g^4 + \cdots\right] \tag{5.57}$$

Rod Oscillator Measurements

The response of the neutron population, as measured by a neutron detector $R(t) \sim n(t)$, to a sinusoidal oscillation of a control rod that produces a sinusoidal reactivity perturbation

$$\rho(t) = \rho_0 \sin\omega t \tag{5.58}$$

can be used to determine a number of neutron kinetics parameters. The response of the neutron population to a sinusoidal reactivity perturbation can be calculated from Eq. (5.45) by first computing the Laplace transform of Eq. (5.58):

$$\rho(s) = \frac{\rho_0\omega}{s^2+\omega^2} = \frac{\rho_0\omega}{(s+i\omega)(s-i\omega)} \tag{5.59}$$

and then Laplace inverting Eq. (5.45), or equivalently, by using Eq. (5.58) in Eq. (5.47), to obtain

$$n_1(t) = n_0\rho_0[|Z(i\omega)|\sin(\omega t+\phi)] + \omega\sum_{j=0}^{6}\frac{e^{s_j t}}{(\omega^2+s_j^2)(dY/ds)_{s_j}} \tag{5.60}$$

where ϕ is the *phase angle*, defined by

$$\tan\phi \equiv \frac{\mathrm{Im}\{Z(i\omega)\}}{\mathrm{Re}\{Z(i\omega)\}} \tag{5.61}$$

The first term in Eq. (5.60) arises from the poles of the reactivity [Eq. (5. 59)] at $s = \pm i\omega$, and the remaining terms arise from the poles of the zero-power transfer function $Z(s)$ [i.e., the roots of the inhour equation $Y(s) = 0$ given by Eq. (5.13)]. For a critical system, the largest root of the inhour equation is $s = 0$, so that after sufficient time the solution given by Eq. (5.60) approaches

$$n_1(t) \simeq n_0\rho_0\left[|Z(i\omega)|\sin(\omega t+\phi) + \frac{1}{\omega\Lambda}\right] \tag{5.62}$$

The average neutron detector response will be $(\rho_0/\omega\Lambda)R_0$, where R_0 is the average detector response before the oscillation began. At high oscillation frequency, the contribution of the first term in Eq. (5.62) to the detector response will average to zero and the detector response will reflect the second term. In both cases, this provides a means for the experimental determination of ρ_0/Λ in terms of the average detector response $\langle R\rangle$:

$$\frac{\rho_0}{\Lambda} = \omega\frac{\langle R\rangle - R_0}{R_0} \tag{5.63}$$

Zero-Power Transfer Function Measurements

By varying the frequency of rod oscillation, ω, the zero-power transfer function, $Z(i\omega)$, can be measured for a reactor or other critical fission chain reacting system by interpreting the detector reading $R(t)$ as

$$R(t) - R_0 = R_0\rho_0\left[|Z(i\omega)|\sin(\omega t + \phi) + \frac{1}{\omega\Lambda}\right] \tag{5.64}$$

Such measurements, when compared with calculation of the transfer function, provide an indirect means of determining or confirming the parameters Λ, β_i, and λ_i. At low frequencies the amplitude of the transfer function approaches

$$|Z(i\omega)| \to \left|\omega\sum_{i=1}^{6}\frac{\beta_i/\beta}{\lambda_i^2}\right| \tag{5.65}$$

for $\omega \ll \lambda_i$, and the phase angle ϕ approaches

$$\tan\phi \to -\sum_{i=1}^{6}\frac{\beta_i/\beta}{\lambda_i}\Bigg/\omega\sum_{i=1}^{6}\frac{\beta_i/\beta}{\lambda_i^2} \tag{5.66}$$

Rossi-α Measurement

The prompt neutron decay constant

$$\alpha \equiv \frac{1}{n}\frac{dn}{dt} = \frac{k(1-\beta)-1}{l} \tag{5.67}$$

can be measured by observing the decay of individual fission reaction chains in succession if the process is continued long enough to observe a statistically significant number of decay chains. Assume that a neutron count from a decay chain is observed at $t = 0$. The probability of another neutron count being observed at a later time t is the sum of the probability of a count from a chain-related neutron, $Q\exp(\alpha t)\Delta t$, plus the probability of a neutron from another chain, $C\Delta t$, where C is the average counting rate:

$$P(t)\,dt = C\,dt + Qe^{\alpha t}\,dt \tag{5.68}$$

We use a statistical argument to determine Q. The probability of a count occurring at t_0 is $F\,dt_0$, where F is just the average fission rate in the system. The probability of another detector count at $t_1 > t_0$ that is chain related to the count at t_0 is

$$P(t_1)dt_1 = \varepsilon \nu_p \mathrm{v}\Sigma_f e^{\alpha(t_1-t_0)}dt_1 \tag{5.69}$$

where ν_p is the number of prompt neutrons per fission and ε is the detector efficiency. The probability of a second chain-related count at $t_2 > t_1$ is

$$P(t_2)dt_2 = \varepsilon(\nu_p - 1)\mathrm{v}\Sigma_f e^{\alpha(t_2-t_0)}dt_2 \tag{5.70}$$

where $(\nu_p - 1)$ takes account of the chain-related fission required to produce the count at t_1. The three probabilities $F\,dt_0$, $P(t_1)dt_1$ and $P(t_2)dt_2$ are treated as independent probabilities. Hence the probability for a count in dt_1 followed by a count in dt_2, both in the chain that produced the count in dt_0, is obtained by multiplying the three probabilities and integrating over $-\infty < t < t_1$:

$$\begin{aligned} P(t_1,t_2)dt_1dt_2 &= \int_{-\infty}^{t_1} F\varepsilon^2\left(\overline{\nu_p^2} - \bar{\nu}_p\right)(\mathrm{v}\Sigma_f)^2 e^{\alpha(t_1+t_2-2t_0)}dt_0dt_1dt_2 \\ &= F\varepsilon^2\left(\overline{\nu_p^2} - \bar{\nu}_p\right)\frac{(\mathrm{v}\Sigma_f)^2}{-2\alpha}e^{\alpha(t_2-t_1)}dt_1dt_2 \end{aligned} \tag{5.71}$$

where an overbar indicates an average over the prompt neutron emission distribution function.

Noting that $\nu_p = k_p\Sigma_a/\Sigma_f = k_p/(\mathrm{v}l\Sigma_f)$ and including the probability $F^2\varepsilon^2dt_1dt_2$ of a random pair of counts, this becomes

$$P(t_1,t_2)dt_1dt_2 = F^2\varepsilon^2dt_1dt_2 + F\varepsilon^2\frac{(\overline{\nu_p^2} - \bar{\nu}_p)k_p^2e^{\alpha(t_2-t_1)}dt_1dt_2}{2\overline{\nu_p^2}(1-k_p)l} \tag{5.72}$$

Since the overall probability of a count in dt_1 is $F\varepsilon dt_1$, we need to normalize this conditional probability by division by $F\varepsilon dt_1$, which yields, upon rescaling time from $t_1 = 0$,

$$P(t_1,t_2)dt_1dt_2 = \frac{\varepsilon(\overline{\nu_p^2} - \bar{\nu}_p)}{\overline{\nu_p^2}}\frac{k_p^2}{2(1-k_p)l}e^{\alpha t}dt \tag{5.73}$$

This is the $Q\exp(\alpha t)dt$ term in Eq. (5.68), so

$$Q = \frac{\varepsilon(\overline{\nu_p^2} - \bar{\nu}_p)}{\overline{\nu_p^2}}\frac{k_p^2}{2(1-k_p)l} \tag{5.74}$$

In a Rossi-α experiment, the function $P(t)$ of Eq. (5.68) is measured by a time analyzer and the random count rate $C\,dt$ is subtracted. The parameter α is then determined from the remaining $Q\exp(\alpha t)dt$ term.

5.7
Reactivity Feedback

Up to this point, we have discussed neutron kinetics—the response of the neutron population in a nuclear reactor or other fission chain reacting system to an external reactivity input—under the implicit assumption that the level of the neutron population does not affect the properties of the system that determine the neutron kinetics, most notably the reactivity. This is the situation when the neutron population is sufficiently small that the fission heat does not affect the temperature of the system (i.e., at zero power). However, in an operating nuclear reactor the neutron population is large enough that any change in fission heating resulting from a change in neutron population will produce changes in temperature, which in turn will produce changes in reactivity, or reactivity feedback. The combined and coupled response of the neutron population and of the temperatures, densities, and displacements of the various materials in a nuclear reactor is properly the subject of reactor dynamics, but the term is commonly used to also include neutron kinetics.

When the neutron population increases, the fission heating increases. Since this heating is deposited in the fuel element, the fuel temperature will increase immediately. An increase in fuel temperature will broaden the effective resonance absorption (and fission) cross section, generally resulting in an increase in neutron absorption and a corresponding reduction in reactivity—the *Doppler effect*. The fuel element will also expand and, depending on the constraints, bend or bow slightly, thus changing the local fuel–moderator geometry and *flux disadvantage factor* (the ratio of the flux in the fuel to the flux in the moderator), thereby producing a change in reactivity. If the increase in fission heating is large enough to raise the fuel temperature above the melting point, fuel slumping will occur, resulting in a large change in the local fuel–moderator geometry and a corresponding change in flux disadvantage factor and fuel absorption, producing a further change in reactivity.

Some of the increased fission heat will be transported out of the fuel element (time constant of tenths of seconds to seconds) into the surrounding moderator/coolant and structure, causing a delayed increase in moderator/coolant and structure temperature. An increase in moderator/coolant temperature will produce a decrease in moderator/coolant density, which causes a change in the local fuel–moderator properties and a corresponding change in both the moderator absorption and the flux disadvantage factor. In addition, a decrease in moderator density will reduce the moderating effectiveness and produce a hardening (shift to higher energies) in the neutron energy distribution, which will change the effective energy-averaged absorption cross sections for the fuel, control elements, and so on. An increase in structure temperature will cause expansion and deformation, producing a change in the local geometry that will further affect the flux disadvantage factor. These various moderator/coolant changes all produce changes in reactivity.

The reduction in moderator/coolant density increases the diffusion of neutrons, and the increase in temperature causes an expansion of the reactor. The effect of

increased diffusion is to increase the leakage, and the effect of increased size is to reduce the leakage, producing offsetting negative and positive reactivity effects. In addition to these internal (to the core) reactivity feedback effects, there are external feedback effects caused by changes in the coolant outlet temperature that will produce changes in the coolant inlet temperature.

Temperature Coefficients of Reactivity

The temperature coefficient of reactivity is defined as

$$\alpha_T \equiv \frac{\partial \rho}{\partial T} = \frac{\partial}{\partial T}\left(\frac{k-1}{k}\right) = \frac{1}{k^2}\frac{\partial k}{\partial T} \simeq \frac{1}{k}\frac{\partial k}{\partial T} \tag{5.75}$$

To gain physical insight into the various physical phenomena that contribute to the reactivity feedback, we first use the one-speed diffusion theory expression for the effective multiplication constant for a bare reactor, but extend it to account for fast fission by including the ratio ε = total fission/thermal fission, to account for the resonance absorption of neutrons during the slowing down to thermal energies by including the resonance escape probability p, and to account for the leakage of fast as well as thermal neutrons by replacing the diffusion length with the migration length M:

$$\begin{aligned} k = k_\infty P_{\mathrm{NL}} &= \frac{\nu\Sigma_f}{\Sigma_a}\frac{1}{1+L^2B^2} = \frac{\nu\Sigma_f}{\Sigma_a^F}\frac{\Sigma_a^F}{\Sigma_a}\frac{1}{(1+L^2B^2)} \\ &= \eta f P_{\mathrm{NL}} \to \eta f \varepsilon p P_{\mathrm{NL}} \end{aligned} \tag{5.76}$$

which allows us to write

$$\alpha_T = \frac{1}{\eta}\frac{\partial \eta}{\partial T} + \frac{1}{\varepsilon}\frac{\partial \varepsilon}{\partial T} + \frac{1}{f}\frac{\partial f}{\partial T} + \frac{1}{p}\frac{\partial p}{\partial T} + \frac{1}{P_{\mathrm{NL}}}\frac{\partial P_{\mathrm{NL}}}{\partial T} \tag{5.77}$$

This formalism lends itself to physical interpretation and can provide quantitative estimates of reactivity coefficients for thermal reactors, but it is not directly applicable to fast reactors. We discuss fast reactor reactivity coefficients in the next section, where a perturbation theory formalism that is more appropriate for the quantitative evaluation of reactivity coefficients in both fast and thermal reactors is introduced. We now discuss reactivity feedback effects on p, f, and P_{NL}; there are also smaller reactivity effects associated with η due to shifts in the thermal neutron energy distribution and associated with ε, which latter are similar to the effects associated with the thermal utilization factor.

Doppler Effect

The resonance capture cross section (one-level Breit–Wigner) is

$$\sigma_\gamma = \sigma_0\sqrt{\frac{E_0}{E}}\frac{\Gamma_\gamma}{\Gamma}\psi(x,\xi) \tag{5.78}$$

where ψ is the Doppler broadening shape function, which takes into account the averaging of the neutron–nucleus interaction cross section over the thermal motion of the nucleus,

$$\psi(x,\xi) = \frac{\xi}{\sqrt{4\pi}} \int_{-\infty}^{\infty} e^{-[(x-y)^2\xi^2/4]} \frac{dy}{1+y^2} \tag{5.79}$$

σ_0 is the peak resonance cross section, Γ_γ and Γ are the capture and total widths of the resonance, $x = (E - E_0)/\Gamma$, $\xi = \Gamma/(4E_0kT/A)^{1/2}$, E and E_0 are the energies of the neutron and of the resonance peak, and A is the mass of the nucleus in amu. The total capture in the resonance is given by the resonance integral

$$I_\gamma \equiv \int \sigma_\gamma(E)\phi(E)dE \tag{5.80}$$

The function ψ broadens with increasing temperature, T, characterizing the motion of the nucleus. A broadening of the ψ function reduces the energy self-shielding in the resonance and increases the resonance integral. Thus an increase in fuel temperature due to an increase in fission heating will cause an increase in the effective capture cross section $\langle\sigma_\gamma\rangle \sim I_\gamma$. A similar result is found for the fission resonances.

In thermal reactors, the Doppler effect is due primarily to epithermal capture resonances in the nonfissionable fuel isotopes (^{232}Th, ^{238}U, ^{240}Pu) and can be estimated by considering the change in resonance escape probability

$$p = e^{-(N_F I_\gamma/\xi\Sigma_p)} \tag{5.81}$$

where $\xi\Sigma_p/N_F$ is the average moderating power per fuel atom, with a sum over resonance integrals for all fuel resonances implied, the function

$$J(\xi,\beta') \equiv \int_0^{\infty} \frac{\psi(x,\xi)}{\psi(x,\xi)+\beta'} dx \tag{5.82}$$

is tabulated in Table 4.3, and $\beta' = (\Sigma_p/N_F)(\Gamma/\sigma_0\Gamma_\gamma)$. The Doppler temperature coefficient of reactivity for a thermal reactor can then be calculated as

$$\alpha_{T_F}^D = \frac{\partial\rho}{\partial T_F} \simeq \frac{1}{k}\frac{\partial k}{\partial T_F} = \frac{1}{p}\frac{\partial p}{\partial T_F} = \ln p\left(\frac{1}{I}\frac{\partial I}{\partial T_F}\right) \tag{5.83}$$

Since the additional fission heating is deposited in the fuel, the fuel temperature, T_F, increases immediately, and the Doppler effect immediately reduces the reactivity. The Doppler effect is a very strong contributor to the safety and operational stability of thermal reactors.

There are useful fits to the total resonance integrals for $^{238}UO_2$ and $^{232}ThO_2$:

$$I(300\text{ K}) = 11.6 + 22.8\left(\frac{S_F}{M_F}\right)$$

$$I(T_F) = I(300\text{ K})\left[1 + \beta''\left(\sqrt{T(\text{K})} - \sqrt{300}\right)\right]$$

$$^{238}\mathrm{UO}_2 : \beta'' = 61 \times 10^{-4} + 47 \times 10^{-4}\left(\frac{S_F}{M_F}\right) \tag{5.84}$$

$$^{232}\mathrm{ThO}_2 : \beta'' = 97 \times 10^{-4} + 120 \times 10^{-4}\left(\frac{S_F}{M_F}\right)$$

where S_F and M_F are surface area and mass of the fuel element. Using this fit, Eq. (5.83) becomes

$$\alpha_{T_F}^D = -\ln\left[\frac{1}{p(300\ \mathrm{K})}\right]\frac{\beta''}{2\sqrt{T_F(\mathrm{K})}} \tag{5.85}$$

Fuel and Moderator Expansion Effect on Resonance Escape Probability

When the fuel temperature increases, the fuel will expand, causing among other things a decrease in the fuel density, which affects the resonance escape probability and contributes an immediate temperature coefficient of reactivity:

$$\alpha_{T_F}^p = \frac{1}{p}\frac{\partial p}{\partial N_F}\frac{\partial N_f}{\partial T_f} = \ln p\left(\frac{1}{N_F}\frac{\partial N_F}{\partial T_F}\right) = -3\theta_F \ln p \tag{5.86}$$

where $(dN/dT)/T = -3(dl/dT)/l = -3\theta$, with θ being the linear coefficient of expansion of the material. Since the fuel density decreases upon expansion, the resonance absorption decreases, and this reactivity coefficient contribution is positive (note that since $p < 1$, $\ln p < 0$).

After the increase in fission heating has been transported out of the fuel element into the coolant/moderator, the moderator temperature, T_M, will increase, which causes the moderator to expand and contributes a delayed temperature coefficient of reactivity:

$$\alpha_{T_M}^p = \frac{1}{p}\frac{\partial p}{\partial N_M}\frac{\partial N_M}{\partial T_M} = -\ln p\left(\frac{1}{N_M}\frac{\partial N_M}{\partial T_M}\right) = 3\theta_M \ln p \tag{5.87}$$

The decreased moderator density reduces the moderating power, reducing the probability that the neutrons will be scattered to energies beneath the resonance, hence increasing the resonance absorption and contributing a negative reactivity coefficient.

Example 5.5: Resonance Escape Probability Fuel Temperature Coefficient for UO_2. The prompt feedback resulting immediately from an increase in power is associated with the increase in fuel temperature, the most significant part of which is due to the change in the resonance escape probability due to the Doppler broadening of resonances, as given by Eq. (5.85), and due to the fuel expansion, as given by Eq. (5.86). For a UO_2 reactor consisting of assemblies of 1-cm-diameter fuel pins of height H in a water lattice with $\Sigma_p/N_F = 100$ and fuel density $\rho = 10$ g/cm^3, $S_F/M_F = \pi dH/\pi(d/2)^2 H\rho = 0.4$, $I(300\ \mathrm{K}) = 11.6 + 22.8 \times 0.4 = 20.72$, and $\beta'' = 61 + 47(S_F/M_F) \times 10^{-4} = 79.8 \times 10^{-4}$. The resonance escape probability at

300 K is $p = \exp(-N_F I/\xi\Sigma_p) = \exp[-20.72/(100 \times 0.948)] = 0.8036$, and $\ln(p) = -0.2186$. The Doppler temperature coefficient of reactivity at 300 K is $\alpha_{TF}^D = \ln(p)\beta''/2T^{1/2} = (-0.2186)(79.8 \times 10^{-4})/(2)(17.32) = -5.036 \times 10^{-5}\Delta k/k$. The linear thermal expansion coefficient for UO_2 is $\theta_F = 1.75 \times 10^{-5}$ K^{-1}, and the fuel expansion contribution to the resonance escape probability temperature coefficient of reactivity is $\alpha_{TF}^p = -3\theta_F \ln(p) = -3(1.75 \times 10^{-5}) \cdot (-0.2186) = 1.148 \times 10^{-5}\Delta k/k$. Thus the total prompt fuel temperature coefficient of reactivity due to the resonance escape probability is $\alpha_{TF}^D + \alpha_{TF}^p = -3.888 \times 10^{-5}\Delta k/k$.

Thermal Utilization

The thermal utilization can be written simply in terms of the effective cell-averaged fuel and moderator absorption cross sections discussed in Section 3.8:

$$f = \frac{\Sigma_{aF}^{\text{eff}}}{\Sigma_{aF}^{\text{eff}} + \Sigma_{aM}^{\text{eff}}} \to \frac{\Sigma_a^F}{\Sigma_a^F + \Sigma_a^M} \tag{5.88}$$

Recalling that $\Sigma \equiv N\sigma$, the reactivity coefficient associated with the thermal utilization has an immediate negative component associated with the fuel temperature increase and a delayed positive contribution associated with the moderator density decrease:

$$\begin{aligned}
\frac{1}{f}\frac{\partial f}{\partial T} &= (1-f)\left[\left(\frac{1}{\sigma_a^F}\frac{\partial \sigma_a^F}{\partial T_F} + \frac{1}{\Sigma_a^F}\frac{\partial \Sigma_a^F}{\partial \xi}\frac{\partial \xi}{\partial T_F} + \frac{1}{N_F}\frac{\partial N_F}{\partial T_F}\right)\right. \\
&\qquad \left. - \left(\frac{1}{\sigma_a^M}\frac{\partial \sigma_a^M}{\partial T_M} + \frac{1}{\Sigma_a^M}\frac{\partial \Sigma_a^M}{\partial \xi}\frac{\partial \xi}{\partial T_M} + \frac{1}{N_M}\frac{\partial N_M}{\partial T_M}\right)\right] \\
&\simeq (1-f)\left[\left(\frac{1}{2T_F} - \frac{1}{\Sigma_a^F}\frac{\partial \Sigma_a^F}{\partial \xi}\frac{\partial \xi}{\partial T_F} + 3\theta_F\right)\right. \\
&\qquad \left. - \left(-\frac{1}{\Sigma_a^M}\frac{\partial \Sigma_a^M}{\partial \xi}\frac{\partial \xi}{\partial T_M} + 3\theta_M\right)\right] \\
&\equiv \alpha_{T_F}^f + \alpha_{T_M}^f
\end{aligned} \tag{5.89}$$

Account has been taken in writing Eq. (5.89) of the fact that the thermal disadvantage factor, ξ, which is used in the definition of effective homogenized fuel and moderator cross sections, will also be affected by a change in temperature. An increase in fuel temperature hardens (makes more energetic) the thermal neutron energy distribution, which reduces the spectrum average of the 1/v thermal fuel cross section and thus reduces the thermal utilization. An increase in the fuel temperature also reduces the fuel density, further reducing the thermal utilization. An increase in moderator temperature has little effect on the moderator cross section but reduces the moderator density, which increases the thermal utilization.

Nonleakage Probability

The nonleakage probability can be represented by

$$P_{\mathrm{NL}} \simeq \frac{1}{1 + M^2 B_g^2} \tag{5.90}$$

Temperature increases can affect the nonleakage probability by changing the characteristic neutron migration length, or the mean distance that a neutron is displaced before absorption, and by changing the size of the reactor. Assuming that both of these effects are associated primarily with changes in the moderator temperature, we write

$$\frac{1}{P_{\mathrm{NL}}} \frac{\partial P_{\mathrm{NL}}}{\partial T_M} = -\frac{M^2 B_g^2}{1 + M^2 B_g^2} \left(\frac{1}{M^2} \frac{\partial M^2}{\partial T_M} + \frac{1}{B_g^2} \frac{\partial B_g^2}{\partial T_M} \right) \tag{5.91}$$

An increase in moderator temperature causes a decrease in moderator density, which affects the migration area as

$$\begin{aligned} \frac{1}{M^2} \frac{\partial M^2}{\partial T_M} &= \frac{1}{D_M} \frac{\partial D_M}{\partial T_M} - \frac{1}{\Sigma_a^M} \frac{\partial \Sigma_a^M (1 - f)}{\partial T_M} \\ &= 6\theta_M + \frac{1}{2T_F} - \frac{1}{1 - f} \frac{\partial f}{\partial T} \end{aligned} \tag{5.92}$$

where we have used $\Sigma_a = \Sigma_a^M + \Sigma_a^F = \Sigma_a^M (1 - f)$.

The geometric buckling $B_g = G/l_R$, where G is a constant depending on geometry (Table 3.3) and l_R is a characteristic physical dimension of the reactor. Thus

$$\frac{1}{B_g^2} \frac{\partial B_g^2}{\partial T_M} = \left(\frac{l_R}{G} \right)^2 \frac{\partial (G/l_R)^2}{\partial T_M} = -2 \left(\frac{1}{l_R} \frac{\partial l_R}{\partial T_M} \right) \tag{5.93}$$

and Eq. (5.91) becomes

$$\begin{aligned} \alpha_{T_M}^{P_{\mathrm{NL}}} &= \frac{1}{P_{\mathrm{NL}}} \frac{\partial P_{\mathrm{NL}}}{\partial T_M} \\ &= \frac{M^2 B_g^2}{1 + M^2 B_g^2} \left(\frac{2}{l_R} \frac{\partial l_R}{\partial T_M} - 6\theta_M - \frac{1}{2T_F} + \frac{1}{1 - f} \frac{\partial f}{\partial T} \right) \end{aligned} \tag{5.94}$$

A decrease in moderator density allows neutrons to travel farther before absorption, which increases the leakage and contributes a negative reactivity coefficient component. Expansion of the reactor means that a neutron must travel farther to escape, which contributes a positive reactivity coefficient component.

Representative Thermal Reactor Reactivity Coefficients

Reactivity coefficients calculated for representative thermal reactors are given in Table 5.2.

Table 5.2 Representative Reactivity Temperature Coefficients in Thermal Reactors

	BWR	PWR	HTGR
Doppler ($\Delta k/k \times 10^{-6}$ K^{-1})	-4 to -1	-4 to -1	-7
Coolant void ($\Delta k/k \times 10^{-6}$/% void)	-200 to -100	—	—
Moderator ($\Delta k/k \times 10^{-6}$ K^{-1})	-50 to -8	-50 to -8	$+1$
Expansion ($\Delta k/k \times 10^{-6}$ K^{-1})	≈ 0	≈ 0	≈ 0

Source: Data from Ref. 3; used with permission of Wiley.

Example 5.6: UO_2 Fuel Heat Removal Time Constant. It is important to emphasize that the temperature reactivity feedback associated with the various mechanisms that have been discussed take place at different times. The feedback associated with changes in the fuel temperature take place essentially instantaneously, since an increase in fission rate produces an immediate increase in fuel temperature. However, the increase in moderator/coolant temperature occurs later, after some of the additional heat is conducted out of the fuel element. The heat balance equation in the fuel element,

$$\rho C\left(\frac{\partial T}{\partial t}\right) = r^{-1}\frac{\partial}{\partial r}\left(\frac{r\kappa\partial T}{\partial r}\right) + q''' \tag{5.95}$$

where ρ is the fuel density, κ the heat conductivity, C the heat capacity, and q''' the volumetric fission heat source, can be used to estimate a time constant characterizing the conduction of heat out of the fuel element to the interface with the coolant/moderator for a fuel pin of radius a, $\tau \approx \rho C a^2/\kappa$.

Typical parameters for a UO_2 fuel element in a thermal reactor are $a = 0.5$ cm, $\kappa = 0.024$ W/cm · K, $\rho = 10.0$ g/cm^3, and $C = 220$ J/kg · K. The heat conduction time constant for heat removal from the fuel into the coolant is $\tau = \rho C a^2/\kappa = (10\text{ g/cm}^3)(220\text{ J/kg} \cdot \text{K})/(0.024\text{ J/s} \cdot \text{cm} \cdot \text{K})(10^3\text{ g/kg}) = 22.9$ s. For a smaller fuel pin characteristic of a fast reactor with $a = 0.25$ cm, the UO_2 fuel time constant would be about 6 s. With a metal fuel instead of UO_2, the heat conductivity is much larger, and the heat removal time constants are on the order of 0.1 to 1.0 s.

Startup Temperature Defect

A reactor is initially started up from a cold condition by withdrawing control rods until the reactor is slightly supercritical, thus producing an exponentially increasing neutron population on a very long period. As the neutron population increases, the fission heating and thus the reactor temperature increase. This increase in temperature produces a decrease in reactivity (almost all reactors are designed to have a negative temperature coefficient) that would cause the neutron population to decrease and the reactor to shut down if the control rods were not withdrawn further to maintain an increasing neutron population. The total amount of feedback reactivity that must be offset by control rod withdrawal during the course of the startup to operating power level is known as the *temperature defect*. The temperature defects

for water-moderated reactors, graphite-moderated reactors, and sodium-cooled fast reactors are about $\Delta k/k = 2\text{–}3 \times 10^{-2}$, 0.7×10^{-2}, and 0.5×10^{-2}, respectively.

5.8 Perturbation Theory Evaluation of Reactivity Temperature Coefficients

Perturbation Theory

The multigroup diffusion equations (Chapter 4) are

$$-\nabla \cdot D_g \nabla \phi_g + \Sigma_{rg}\phi_g = \sum_{g' \neq g}^{G} \Sigma_{g' \to g}\phi_{g'} + \frac{1}{k}\chi_g \sum_{g'=1}^{G} \nu\Sigma_{fg'}\phi_{g'},$$
$$g = 1, \ldots, G \tag{5.96}$$

where $\Sigma_{g' \to g}$ is the cross section for scattering a neutron from group g' to group g, Σ_{rg} is the removal cross section for group g, which is equal to the absorption cross section plus the cross section for scattering to all other groups, χ_g is the fraction of the fission neutrons in group g, D_g and $\nu\Sigma_{fg}$ are the diffusion coefficient and the nu-fission cross section in group g, and ϕ_g is the neutron flux in group g.

We now consider a perturbation in materials properties (e.g., as would be caused by a change in local temperature) such that the reactor is described by an equation like Eq. (5.96), but with $D_g \to D_g + \Delta D_g$, $\Sigma_g \to \Sigma_g + \Delta\Sigma_g$, where the Δ terms include changes in densities, changes in the energy averaging of the cross-section data and energy self-shielding, changes in spatial self-shielding, and changes in geometry. If we assume that the perturbation in materials properties is sufficiently small that it does not significantly alter the group fluxes, we can multiply the unperturbed and perturbed equations by ϕ_g^+, subtract the two, integrate over the volume of the reactor, and sum the resulting equations for all groups to obtain the perturbation theory estimate for the change in reactivity associated with the perturbation in material properties:

$$\frac{\Delta k}{k} \simeq \sum_{g=1}^{G} \int dr \left[\phi_g^+ \nabla \cdot (\Delta D_g \nabla \phi_g) - \phi_g^+ \Delta\Sigma_{rg}\phi_g + \phi_g^+ \sum_{g' \neq g}^{G} \Delta\Sigma_{g' \to g}\phi_{g'} \right.$$
$$\left. + \phi_g^+ \chi_g \sum_{g'=1}^{G} \Delta(\nu\Sigma_{fg'})\phi_{g'} \right]$$
$$\div \sum_{g=1}^{G} \int dr \left(\phi_g^+ \chi_g \sum_{g'=1}^{G} \nu\Sigma_{fg'}\phi_{g'} \right) \tag{5.97}$$

The quantity ϕ_g^+, the importance of neutrons in group g in producing a subsequent fission event, is discussed in Chapter 13. This expression, together with the

subsidiary calculation of the $\Delta\Sigma_g$ and ΔD_g terms, including all the effects mentioned above, provides a practical means for the quantitative evaluation of reactivity coefficients in nuclear reactors.

Example 5.7: Reactivity Worth of Uniform Change in Thermal Absorption Cross Section. With the assumption that all of the fission occurs in the thermal group, the reactivity worth of a uniform change in thermal absorption cross section in a uniform thermal reactor is $\Delta k/k = \Delta\Sigma_a^{\text{th}} I_{\text{th}}/\nu\Sigma_j^{\text{th}} I_{\text{th}} \approx \Delta\Sigma_a^{\text{th}}/\Sigma_a^{\text{th}}$, because I_{th}, the integral over the reactor of the product of the thermal group importance function and flux, appears in both the numerator and denominator, and because in a critical reactor $\Sigma_a^{\text{th}} \approx \nu\Sigma_f^{\text{th}}$.

We now discuss some fast reactor reactivity coefficients that could not be treated by the more approximate method of the preceding section, although we emphasize that this perturbation theory calculation is also used for thermal reactor reactivity coefficient evaluation.

Sodium Void Effect in Fast Reactors

The reactivity change that occurs when sodium is voided from a fast reactor can be separated into leakage, absorption, and spectral components. The *leakage* and *spectral components* correspond to the first (ΔD_g) and third ($\Delta\Sigma_{g'\to g}$) terms, respectively, in Eq. (5.97). The *absorption component* corresponds to the second ($\Delta\Sigma_{rg}$) and fourth ($\Delta\nu\Sigma_f$) terms in Eq. (5.97), although the change in fission cross section is usually small and therefore neglected, and this component is usually referred to as the *capture component*. The spectral and capture components are normally largest in the center of the core, where the neutron flux and importance function are largest, and the leakage component is normally largest in the outer part of the core, where the flux gradient is largest.

The magnitude of the sodium void coefficient varies directly with the ratio of the number of sodium atoms removed to the number of fuel atoms present. The spectral component of the sodium void coefficient is generally positive, is more positive for ^{239}Pu than for ^{235}U, and becomes increasingly positive as fissile material concentration decreases relative to sodium content. The capture component tends to become more positive with softer neutron spectra because of the 2.85-keV resonance in ^{23}Na, hence to become more positive with increasing sodium concentration relative to fuel concentration. The negative leakage component is generally smaller than the other two components, although the leakage component can be enhanced by the choice of geometrical configuration. As a result, the overall reactivity effect of voiding the central part of the core is positive, and may be positive for voiding of the entire core. This poses a serious safety concern that must be offset by proper design to ensure that other negative reactivity coefficients are dominant.

Doppler Effect in Fast Reactors

In fast reactors, the neutron energy spectrum includes the resonance regions of both the fissionable (^{235}U, ^{233}U, ^{239}Pu, ^{241}Pu) and nonfissionable (^{232}Th, ^{238}U,

^{240}Pu) fuel isotopes. The Doppler effect in fast reactors is due almost entirely to resonances below about 25 keV. An increase in fuel temperature will produce an increase in both the fission and absorption cross sections, and the resulting change in reactivity can be positive or negative, depending on the exact composition. The temperature coefficient of reactivity can be estimated from

$$\frac{\partial k}{\partial T_F} = \int N_F \left[\phi_f^+ \frac{\partial \sigma_f}{\partial T_F} - \phi^+(E) \left(\frac{\partial \sigma_\gamma}{\partial T_F} + \frac{\partial \sigma_f}{\partial T_F} \right) \right] \phi(E) dE$$
$$\simeq N_F \int \frac{1}{\nu} \frac{\partial \sigma_f}{\partial T_F} (\nu - 1 - \alpha) \phi(E) dE \tag{5.98}$$

where N_F is the density of fuel nuclei (sum over species implied), $\phi^+(E)$ and ϕ_f^+ are the importance of a neutron at energy E and of a fission neutron (i.e., the number of fissions the neutron subsequently produces). Since in a critical system each neutron will on average produce $1/\nu$ fissions, $\phi^+ \approx \phi_f^+ \approx 1/\nu$ is used in the second form of the estimate, and $\alpha \equiv \sigma_\gamma / \sigma_f$ has also been used. Since α generally decreases with increasing neutron energy (Chapter 2), the reactivity change will tend to be more positive/less negative for metal-fueled cores with a relatively hard spectrum. The oxygen in UO_2 fuel softens (makes less energetic) the energy spectrum and thereby makes the reactivity change more negative/less positive. Detailed design calculations, using methods benchmarked against critical experiments, indicate that in larger reactors with a high fertile-to-fissile ratio the Doppler coefficient is sufficiently negative to provide a prompt shutdown mechanism in the event of excess fission heating of the fuel.

Fuel and Structure Motion in Fast Reactors

The increased fission heating coincident with an increase in the neutron population causes the fuel to expand radially and axially and to distort (e.g., bow) due to constraints. The expanding fuel first compresses, then ejects, sodium. The additional fission heat is transferred to the structure, producing a delayed expansion and distortion of the structure. The radial expansion, which is cumulative from the core center outward, results in a general outward radial movement of the fuel and in an expansion of the size of the reactor. The reactivity effect of this fuel and structure motion is highly dependent on the details of the design. However, a few simple estimates provide a sense of the magnitude of the effects.

Example 5.8: Reactivity Effects of Fuel and Structure Expansion. Radial motion of the fuel by an amount Δr from an initial radial location r causes a reduction in local fuel density which varies as r^2, leading to a local density change $\Delta N_F / N_F \approx (r^2 - (r + \Delta r)^2 / r^2 \approx -2\Delta r / r$. Axial fuel expansion leads to linear fuel density decreases. The overall expansion reactivity coefficient is a combination of the negative effect of reduced fuel density and the positive effect of increased core size, hence reduced leakage. An overall expansion reactivity coefficient is of the form

$$\alpha_{T_M}^{\text{exp}} = \left(a \frac{\Delta R}{R} + b \frac{\Delta N_F}{N_F} \right)_{\text{radial}} + \left(c \frac{\Delta H}{H} + d \frac{\Delta N_F}{N_F} \right)_{\text{axial}} \tag{5.99}$$

Table 5.3 Reactivity Coefficients in a 1000-MWe Oxide-Fueled Fast Reactor

	Temperature $\Delta k/k \times 10^{-6}$ °C^{-1}	Power: $\Delta k/k \times 10^{-6}$ MW^{-1}
Sodium expansion core	+3.0	+0.085
Sodium expansion reflector	−1.6	−0.081
Doppler	−3.2	−0.628
Radial fuel pin expansion	+0.4	+0.117
Axial core expansion	−4.1	−0.181
Radial core expansion	−6.8	−0.182

Source: Data from Ref. 9; used with permission of American Nuclear Society.

where, for the example of a 1000-MWe UO_2 reactor with H/D = 0.6, the constants are ($a = 0.143$, $b = 0.282$, $c = 0.131$, $d = 0.281$).

Fuel Bowing

Fuel distortion (e.g., bowing) is very much a function of how the fuel is constrained. The calculated reactivity effect of inward bowing in the metal fueled EBR-II was $\Delta k/k \approx -0.35\Delta V/V \approx -0.7\Delta R/R \approx 0.0013$. This predicted positive reactivity due to bowing exceeded the combined negative reactivity from all other effects at full flow and intermediate power, suggesting the possibility of a positive reactivity coefficient over the intermediate power range, consistent with experimental observation.

Representative Fast Reactor Reactivity Coefficients

Reactivity coefficients calculated for a representative fast reactor design are given in Table 5.3.

5.9 Reactor Stability

Reactor Transfer Function with Reactivity Feedback

Since the reactor power is related directly to the neutron population, we can rewrite the neutron kinetics equations, in particular Eq. (5.39), in terms of the power, $P = E_f n v \nu \Sigma_f \cdot \text{Vol}$, where E_f is the energy release per fission. If we expand the power about the equilibrium power P_0 as $P(t) = P_0 + P_1(t)$ and limit consideration to the situation $|P_1/P_0| \ll 1$, we find that

$$\frac{dP_1(t)}{dt} = \frac{1}{\Lambda}\left\{\rho(t)P_0 + \int_0^\infty d\tau \beta D(\tau)[P_1(t-\tau) - P_1(t)]\right\} \tag{5.100}$$

Representing the reactivity as the sum of an external reactivity, ρ_{ex}, such as may be caused by control rod motion, and a feedback reactivity, ρ_f, caused by the inherent reactivity feedback mechanisms discussed in the preceding two sections, the total reactivity may be written

$$\begin{aligned}\rho(t) &= \rho_{ex}(t) + \rho_f(t) \\ &= \rho_{ex}(t) + \int_{-\infty}^{t} f(t-\tau) P_1(\tau) d\tau \\ &= \rho_{ex}(t) + \int_{0}^{\infty} f(\tau) P_1(t-\tau) d\tau \end{aligned} \tag{5.101}$$

where $f(t-\tau)$ is the feedback kernel that relates the power deviation $P_1 = P - P_0$ at time $t-\tau$ to the resulting reactivity at time t.

Using the last form of Eq. (5.101) in Eq. (5.100), Laplace transforming (equivalently, assuming an e^{st} time dependence), and rearranging yields a transfer function, $H(s)$, relating the external reactivity input to the power deviation from equilibrium:

$$P_1(s) = \frac{Z(s)}{1 - P_0 F(s) Z(s)} P_0 \rho_{ex}(s) \equiv H(s) P_0 \rho_{ex}(s) \tag{5.102}$$

This new transfer function contains the zero-power transfer function, $Z(s)$, which relates the prompt and delayed neutron response to the external reactivity, and the feedback transfer function, $F(s)$, which relates the feedback reactivity to the power deviation $P_1 = P - P_0$:

$$\rho_f(s) = F(s) P_1(s) \tag{5.103}$$

Note that when $P_0 \to 0$, $H(s) \to Z(s)$.

The linear stability of a nuclear reactor can be determined by locating the poles of $H(s)$ in the complex s-plane. This follows from noting that when Eq. (5.102) is Laplace inverted, the solutions for $P_1(t) \sim \exp(s_j t)$, where the s_j are the poles of $H(s)$. Any poles located in the right half of the complex s-plane (i.e., with a positive real part) indicate a growing value of $P_1(t)$—an instability. Since $Z(s)$ appears in the numerator and denominator of $H(s)$, its poles (the roots of the inhour equation) cancel in $H(s)$, and the poles of $H(s)$ are the roots of

$$1 - P_0 F(s) Z(s) = 0 \tag{5.104}$$

We can anticipate from Eq. (5.104) that the poles of $H(s)$, hence the linear stability of the reactor, will depend on the equilibrium power level, P_0.

Stability Analysis for a Simple Feedback Model

To determine the roots of Eq. (5.104), we must first specify a feedback model in order to determine the feedback transfer function, $F(s)$. We consider a two-

temperature model in which the deviation in the fuel temperature from the equilibrium value satisfies

$$\frac{dT_F(t)}{dt} = a\,P_1(t) - \omega_F T_F(t) \tag{5.105}$$

where a involves the heat capacity and density of the fuel and ω_F is the inverse of the heat transfer time constant of the fuel element (i.e., the time constant for removal of heat from the fuel element into the coolant/moderator). The temperature deviation about the equilibrium value in the coolant/moderator satisfies

$$\frac{dT_M(t)}{dt} = bT_F(t-\Delta t) - \omega_M T_M(t) \tag{5.106}$$

where b involves the mechanism governing the response of the coolant/moderator temperature to a change in the fuel temperature, ω_M is the inverse of the heat removal time constant for the moderator, and for the sake of generality we assume that the coolant mass flow rate is varied in response to the fuel temperature at an earlier time $(t-\Delta t)$. The same model could be applied to any two-temperature representation of a reactor core. For example, we could consider T_F to be the temperature of a simultaneously heated fuel–coolant region and T_M to represent the temperature of the structure in a fast reactor model. Writing

$$\rho(t) = \rho_{\text{ex}}(t) + \alpha_F T_F(t) + \alpha_M T_M(t) \equiv \rho_{\text{ex}}(t) + \int_0^t f(t-\tau)P_1(\tau)d\tau \tag{5.107}$$

defines the feedback kernel, $f(t-\tau)$, where $T_F(t)$ and $T_M(t)$ are deviations from the equilibrium temperatures.

Laplace transforming these three equations, using the convolution theorem, and combining leads to identification of the feedback transfer function:

$$F(s) = \frac{X_F}{1+s/\omega_F} + \frac{X_M e^{-s\Delta t}}{(1+s/\omega_F)(1+s/\omega_M)} \tag{5.108}$$

where $X_F = a\alpha_F/\omega_F$ and $X_M = (ab\alpha_M/\omega_F\omega_M)$ are the steady-state reactivity power coefficient for the fuel and coolant/moderator, respectively. Using the zero-power transfer function, $Z(s)$, of Eq. (5.46), but in the one-delayed neutron group approximation, and the feedback transfer function, $F(s)$, of Eq. (5.108), Eq. (5.104) for the poles of the reactor transfer function with feedback, $H(s)$, becomes

$$1 - \frac{P_0}{s[\Lambda + \beta/(s+\lambda)]}\left[\frac{X_F}{1+s/\omega_F} + \frac{X_M e^{-s\Delta t}}{(1+s/\omega_F)(1+s/\omega_M)}\right] = 0 \tag{5.109}$$

There are a number of powerful mathematical techniques from the field of linear control theory (Nyquist diagrams, root-locus plots, Routh–Hurwitz criterion, iterative root finding methods, etc.) for finding the roots of Eq. (5.109), or of the more complex equations that would result from more detailed reactivity feedback models. Some simplification results from limiting attention to growth rates that are

small compared to the inverse neutron generation time ($s \ll \Lambda^{-1}$), allowing neglect of the Λ term. We now consider two additional approximations which allow us to obtain valuable physical insights.

If we set $X_M \sim \alpha_M = 0$ (i.e., neglect the coolant/moderator feedback), Eq. (5.109) can be solved analytically to obtain

$$s_{\pm} = \frac{1}{2}\omega_F \left(\frac{P_0 X_F}{\beta} - 1 \right) \left[1 \pm \sqrt{1 + \frac{4(P_0 X_F/\beta)(\lambda/\omega_F)}{(P_0 X_F/\beta - 1)^2}} \right] \tag{5.110}$$

If the fuel power coefficient is positive ($X_F \sim \alpha_F > 0$), the term under the radical is positive and greater than unity, both roots are real, and one root is positive, indicating an instability. If the fuel power coefficient is negative ($X_F \sim \alpha_F < 0$), the real parts of both roots are negative, indicating stability.

Threshold Power Level for Reactor Stability

If we retain X_M finite but restrict our consideration to instabilities with growth rates much less than the inverse fuel heat removal time constant, $s \ll \omega_F$, and set the time delay to zero, $\Delta t = 0$, we can again solve Eq. (5.109) analytically for the poles of the reactor transfer function, $H(s)$:

$$s_{\pm} = -\frac{1}{2}\omega_M \frac{1 - \frac{P_0 X_F}{\beta}\left(\frac{X_M}{X_F} + 1 + \frac{\lambda}{\omega_M}\right)}{1 - \frac{P_0 X_F}{\beta}} \times \left[1 \pm \left\{ 1 + \frac{4\left(\frac{\lambda}{\omega_M}\right)\left(\frac{P_0 X_F}{\beta}\right)\left(1 - \frac{P_0 X_F}{\beta}\right)}{\left[1 - \frac{P_0 X_F}{\beta}\left(\frac{X_M}{X_F} + 1 + \frac{\lambda}{\omega_M}\right)\right]^2} \right\}^{1/2} \right] \tag{5.111}$$

This expression reveals the existence of a threshold equilibrium power level, P_0, above which a reactor becomes unstable. As $P_0 \to 0$, the two roots approach 0 and $-\omega_M$, a marginally stable condition, and do not depend on the reactivity power coefficients X_M and X_F. As P_0 increases, the nature of the solution depends on X_M and X_F. Suppose that the fuel power coefficient is positive, $X_F > 0$, and the moderator power coefficient is negative, $X_M < 0$; this situation might arise, for example, in a fast reactor when X_F represents the combined Doppler, fuel expansion, and sodium void coefficients of the fuel–coolant mixture and X_M represents the structure expansion coefficient. Taking $X_F/X_M = -\frac{1}{2}$ and $\omega_M = \frac{1}{4}$, the roots of Eq. (5.111) are plotted as a function of $|X_M|P_0/\beta$ (denoted at P_0) in Fig. 5.4. As P_0 increases from zero, the marginally stable ($s = 0$) root moves into the left-half complex s-plane and the ($s = \omega_M$) root becomes less negative, indicating that the reactor would be stable. At $|X_M|P_0/\beta = 0.0962$, the roots become complex conjugates with a real part that increases with P_0. At $|X_M|P_0/\beta > \frac{2}{3}$, the real part of the two roots becomes positive, indicating that the reactor would become unstable above a certain threshold operating power level. At $|X_M|P_0/\beta > 1.664$, the roots become real and positive, with one increasing and the other decreasing with increasing P_0, continuing to indicate instability.

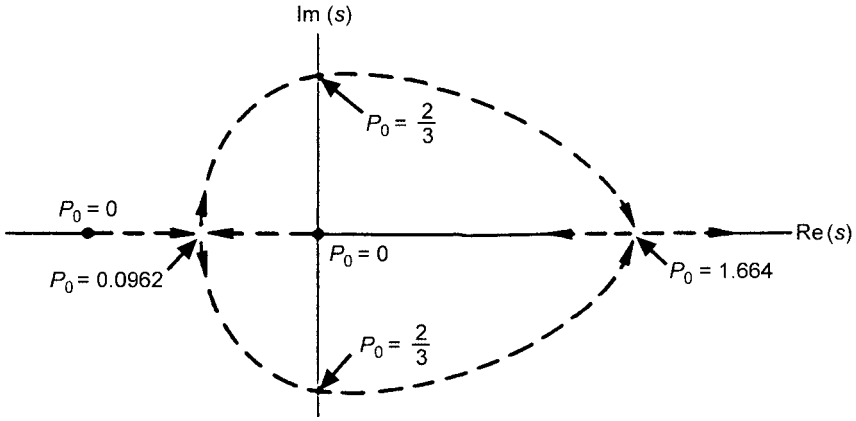

Fig. 5.4 Characteristic roots s_+ and s_- of Eq. (5.111) as a function of critical power level P_0 ($|X_M|P_0/\beta$) ($X_F > 0, X_F/X_M = -\frac{1}{2}, W_M = \frac{1}{4}S$). (From Ref. 8; used with permission of Van Nostrand.)

The total power coefficient at steady state is negative ($F(0) = X_F + X_M < 0$), but the reactor in this example was unstable above a certain threshold power level. The positive fuel power feedback was instantaneous because the fuel temperature increases instantaneously in response to an increase in fission heating. However, the coolant/moderator temperature does not increase instantaneously because of moderator heat removal, but increases on a time scale governed by the moderator heat removal time constant ω_M^{-1} following a change in fuel temperature, as may be seen by solving Eq. (5.106) for a step increase ΔT_F at $t = 0$:

$$\Delta T_M = \begin{cases} 0, & t < \Delta t \\ \dfrac{b\Delta T_F}{\omega_M}(1 - e^{-\omega_M(t+\Delta t)}), & t \geq \Delta t \end{cases} \tag{5.112}$$

The delay of the moderator temperature response to an increase in the temperature of the fuel was neglected; its inclusion would contribute further to the possibility of instabilities. It is clear that heat removal time constants play an important role in the stability of a reactor.

The two-temperature feedback model can be generalized to investigate the stability of a variety of different feedback models that can be characterized by a fast (f)- and a slow (s)- responding temperature. For a fast temperature response that was either prompt ($\omega_f = 0$) or zero ($X_f = 0$) plus a slow temperature response with a finite time constant ($\omega_s \neq 0$) determined either by heat conduction or heat convection, the results are given in Table 5.4.

More General Stability Conditions

A necessary condition for stability is

$$F(0) = \int_0^\infty f(t)dt < 0 \tag{5.113}$$

Table 5.4 Instability Conditions for Some Simple Two-Temperature Feedback Models

Reactivity Coefficients				
Fast ($\omega_f = 0$)	**Slow ($\omega_s \neq 0$)**	**Heat Removal**	$F(s)$	**Instability**
$X_f = 0$	$X_s < 0$	Conduction	$\frac{X_s}{1+s/\omega_s}$	None
$X_f = 0$	$X_s < 0$	Convection	$X_s e^{-s/\omega_s}$	$P_0 > P_{\text{thresh}}$
$X_f > 0$	$X_s < 0$	Conduction	$X_f + \frac{X_s}{1+s/\omega_s}$	$P_0 > P_{\text{thresh}}$
$X_f < 0$	$X_s < 0$	Conduction	$X_f + \frac{X_s}{1+s/\omega_s}$	None
$X_f > 0$	$X_s < 0$	Convection	$X_f + X_s e^{-s/\omega_s}$	$P_0 > P_{\text{thresh}}$
$X_f < 0$	$X_s < 0$	Convection	$X_f + X_s e^{-s/\omega_s}$	$P_0 > P_{\text{thresh}}$
$X_f = 0$	$X_{s1} < 0$	Convection	$X_{s1} e^{-s/\omega_{s1}} + \frac{X_{s2}}{1+s/\omega_{s2}}$	$P_0 > P_{\text{thresh}}$
	$X_{s2} <$ or > 0	Conduction		

Source: Data from Ref. 9; used with permission of American Nuclear Society.

However, this is not a sufficient condition, as the analysis above, in which $F(0) = X_F + X_M < 0$, demonstrates. The result discussed in the preceding example suggests a useful generalization—a reactor is on the verge of becoming unstable when the transfer function, $H(s)$, has a pole with purely imaginary s [i.e., when Eq. (5.104) has a purely imaginary root $s = i\omega$]. Except for values of ω for which $Z(i\omega) = 0$, Eq. (5.104), which determines the poles of the transfer function, can be rewritten in the case $s = i\omega$:

$$G(i\omega) = \frac{1}{Z(i\omega)} - P_0 F(i\omega) = i\omega\Lambda + \sum_{j=1}^{6} \frac{\beta_j i\omega}{i\omega + \lambda_j} - P_0 F(i\omega) = 0 \qquad (5.114)$$

If this equation has a solution, it corresponds to a condition for which the reactor is on the verge of instability. A necessary condition for a solution is that $Z^{-1}(i\omega)$ and $F(i\omega)$ have the same ratio of real to imaginary parts (i.e., the same phase). If $Z^{-1}(i\omega)$ and $F(i\omega)$ do have the same phase at some $\omega = \omega_{\text{res}}$, there will be some value of P_0 for which Eq. (5.114) has a solution. If this value of P_0 is physically reasonable ($P_0 \geq 0$), there is instability onset at this (P_0, ω_{res}) condition. The real and imaginary parts of $1/Z(i\omega)$ are

$$\begin{aligned} \text{Re}\left\{\frac{1}{Z(i\omega)}\right\} &= \sum_{j=1}^{6} \frac{\omega^2 \beta_j}{\omega^2 + \lambda_j^2} \\ \text{Im}\left\{\frac{1}{Z(i\omega)}\right\} &= \omega\Lambda + \sum_{j=1}^{6} \frac{\omega \beta_j \lambda_j}{\omega^2 + \lambda_j^2} \end{aligned} \qquad (5.115)$$

which are both real and positive, thus are in the upper right quadrant of the complex plane. Therefore, a necessary condition for $G(i\omega) = 0$ to have a solution is that

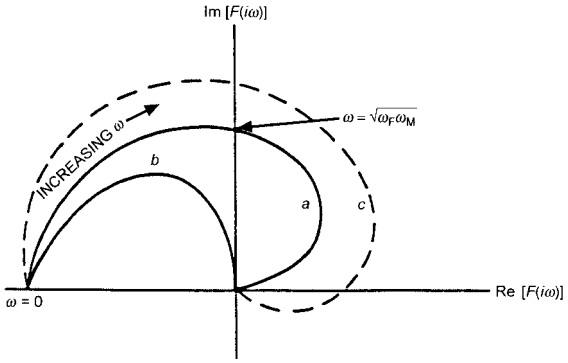

Fig. 5.5 Plot of $R = \mathrm{Re}\{F(i\omega)\} + iI\{F(i\omega)\}$ of Eq. (5.108) with $\Delta t = 0$: case (a) $X_F = 0$, $X_M < 0$; case (b), $X_F < 0$, $X_M < 0$; case (c), $|X_M| > X_F > 0$, $X_M < 0$. (From Ref. 8; used with permission of Van Nostrand.)

the real and imaginary parts of the feedback transfer function, $F(i\omega)$, also lie in the same quadrant (i.e., both be real and positive). Hence a necessary condition for an instability is

$$\mathrm{Re}\{F(i\omega)\} > 0 \quad \text{and} \quad \mathrm{Im}\{F(i\omega)\} > 0 \tag{5.116}$$

We now consider the example above with the simple feedback model of Eqs. (5.105) to (5.108), but with the delay term $\Delta t = 0$. The qualitative behavior of the real and imaginary parts of $F(i\omega)$ of Eq. (5.108) are plotted in Fig. 5.5 for three different cases, all of which have a negative moderator power coefficient, $X_M < 0$. Case (a) corresponds to no reactivity feedback from the fuel ($X_F = 0$); the instability criterion of Eq. (5.116) is satisfied for $\omega > (\omega_M \omega_f)^{1/2}$, even though the steady-state power coefficient $X(0) = X_M < 0$. For case (b), with a sufficiently large negative value of the fuel power coefficient, $X_F < 0$, the criterion of Eq. (5.116) is never satisfied and the reactor is stable. In case (c), the fuel reactivity power coefficient is positive but smaller in magnitude than the negative moderator reactivity power coefficient, $|X_M| > |X_F| > 0$, which is the situation leading to the solution of Eq. (5.111); the reactor can become unstable, as found above from examination of the roots given by Eq. (5.111).

A sufficient condition for unconditional stability (i.e., no power threshold) has been shown to be

$$\mathrm{Re}\{F(i\omega)\} = \int_0^\infty f(t)\cos(\omega t)dt \leq 0 \tag{5.117}$$

which is a requirement that the phase angle of the feedback transfer function, $-F(s)$, along the $i\omega$-axis is between $-90° < \phi < +90°$; thus the feedback response is negative and less than 90° out of phase with the power change that produced it. This phase constraint places constraints on the time delays. This sufficient criterion for stability has been found to be over restrictive, however.

Table 5.5 Sufficient Conditions for Unconditional Stability of Two-Temperature Feedback Models

Reactivity Coefficients	$F(i\omega)$	Stability Criterion
Coupled prompt X_f, conduction X_s	$X_f + \frac{X_s}{1+i\omega/\omega_s}$	$X_f \le 0$ and $X_f + X_s < 0$
Uncoupled conduction X_f and X_s	$\frac{X_f}{1+i\omega/\omega_f} + \frac{X_s}{1+i\omega/\omega_s}$	$X_f + X_s \le 0$, $X_f\omega_f + X_s\omega_s < 0$, and $X_f\omega_f^2 + X_s\omega_s^2 \le 0$
Coupled conduction X_f and X_s	$\frac{X_f}{1+i\omega/\omega_f} + \frac{X_s}{(1+i\omega/\omega_f)(1+i\omega/\omega_s)}$	$X_f < 0$, $X_f + X_s \le 0$, and $X_f\omega_f - X_s\omega_s \le 0$
Coupled prompt X_f, convection X_s	$X_f + X_s e^{-i\omega/\omega_s}$	$X_f < 0$ and $-X_f \ge \lvert X_s \rvert$
Coupled conduction X_f, convection X_s	$\frac{X_f}{1+i\omega/\omega_f} + \frac{X_s e^{-i\omega/\omega_s}}{1+i\omega/\omega_s}$	Never unconditionally stable

The unconditional stability sufficient condition of Eq. (5.117) has been used to determine unconditional stability criteria for a variety of feedback models that can be characterized by a fast (f) and a slow (s) responding temperature. The fast temperature response was either prompt ($\omega_f = 0$) or determined by heat conduction, and the slow temperature response was with a finite time constant ($\omega_s \neq 0$) determined by either heat conduction or heat convection. The results are given in Table 5.5.

Power Coefficients and Feedback Delay Time Constants

It is clear from the previous discussion that the reactivity temperature coefficients actually enter the analysis as reactor power coefficients, associated with which there are time delays related to heat transfer and removal time constants, and that the results of the analysis are dependent on the delay times as well as on the temperature coefficients. We can generalize the two-temperature model to define a general reactor power coefficient:

$$X(t) = \sum_j \left(\frac{\partial \rho}{\partial T_j} \frac{\partial T_j(t)}{\partial P} + \frac{\partial \rho}{\partial T_j'} \frac{\partial T_j'(t)}{\partial P} \right) \tag{5.118}$$

where $\partial\rho/\partial T_j$ are the reactivity temperature coefficients corresponding to a change in local temperature T_j. The quantities $\partial\rho/\partial T_j'$ are reactivity temperature gradient coefficients denoting the change in reactivity due to a change in temperature gradient (e.g., as would produce bowing of a fuel element). These reactivity coefficients can be calculated as discussed in the two preceding sections. The quantities $\partial T_j/\partial P$ and $\partial T_j'/\partial P$ are the time-dependent changes in local temperature and temperature gradients resulting from a change in reactor power and must be cal-

culated from models of the distributed temperature response to a change in reactor power.

The time constants that determine the time delays in the various local temperature responses to a power increase depend on the specific reactor design. Some simple estimates suffice to establish orders of magnitude. The time constant for heat transfer out of a fuel pin of radius r or plate of thickness r, density ρ, heat capacity C, and thermal conductivity κ is $\tau_f = \rho C r^2/\kappa$, which generally varies from a few tenths to a few tens of seconds. The effect of cladding and the surface film drop is to increase the time constant for the fuel element. The lumped time constant for the coolant temperature is $\tau_c = C_c/h + (Z/2\mathrm{v})(1 + C_f/C_c)$, where C_c and C_f are the heat capacities per unit length of the coolant and fuel, respectively, h is the heat transfer coefficient between fuel and coolant, Z is the core height, and v is the coolant flow speed. Typical values of τ_c vary from a few tenths to a few seconds.

5.10 Measurement of Reactor Transfer Functions

Measurement of the reactor transfer function provides useful information about a reactor. A measurement at low power can identify incipient instabilities which produce peaks in the transfer function. Provided that the feedback mechanisms do not change abruptly with power, the low-power transfer function measurements can identify conditions that would be hazardous at high power, thus allowing for their correction. Information about the feedback mechanisms can be extracted from measurement of the amplitude and phase of the transfer function. Any component malfunction that altered the heat removal characteristics of the reactor would affect the transfer function, so periodic transfer function measurements provide a means to monitor for component malfunction.

Rod Oscillator Method

The sinusoidal oscillation of a control rod over a range of frequencies can be used to measure the transfer function, as described in Section 5.6. The results of Eqs. (5.60) to (5.64) apply to a reactor with feedback when $n_0 Z(i\omega)$ is replaced by $P_0 H(i\omega)$. There are some practical problems in measuring the transfer function with rod oscillation. There will be noise in the detector response, which will require a sufficiently large reactivity oscillation for the detector response to be separable from the noise, and nonlinear effects [i.e., the term ρn_1 which was neglected in Eq. (5.42)] may invalidate the interpretation. Furthermore, the oscillation will not be perfectly sinusoidal, and it will be necessary to Fourier analyze the detector response to isolate the fundamental sinusoidal component.

Correlation Methods

It is possible to measure the reactor transfer function with a nonperiodic rod oscillation. Consider the inverse Laplace transform of Eq. (5.102):

$$P_1(t) = \int_{-\infty}^{t} \rho_{ex}(\tau)h(t-\tau)d\tau = \int_{0}^{\infty} \rho_{ex}(t-\tau)h(\tau)d\tau \tag{5.119}$$

which relates the relative power variation from equilibrium $[P_1/P_0 = (P - P_0)/P_0]$ to the time history of the external reactivity—the rod oscillation in this case—including the effect of feedback. The kernel $h(t)$ is the inverse Laplace transform of the transfer function, $H(s)$. The cross correlation between the external reactivity and the power variation is defined as

$$\phi_{\rho P} \equiv \frac{1}{2T}\int_{-T}^{T} \rho_{ex}(t)P_1(t+\tau)dt = \frac{1}{2T}\int_{-T}^{T} \rho_{ex}(t-\tau)P_1(t)dt \tag{5.120}$$

where T is the period if ρ_{ex} and P_1 are periodic and T goes to infinity if not.

Using Eq. (5.119) in Eq. (5.120) yields

$$\begin{aligned}\phi_{\rho P} &= \frac{1}{2T}\int_{-T}^{T} \rho_{ex}(t-\tau)\left[\int_{0}^{\infty} \rho_{ex}\big(t-t'\big)h\big(t'\big)dt'\right]dt \\ &= \int_{0}^{\infty} h(t')\left[\frac{1}{2T}\int_{-T}^{T} \rho_{ex}(t-\tau)\rho_{ex}\big(t-t'\big)dt\right]dt' \\ &\equiv \int_{0}^{\infty} h(t')\phi_{\rho\rho}(\tau-t')dt'\end{aligned} \tag{5.121}$$

where $\phi_{\rho\rho}$ is the reactivity autocorrelation function. Taking the Fourier transform of Eq. (5.121) yields an expression for the transfer function

$$H(-i\omega) = \mp\frac{\mathcal{F}\{\phi_{\rho P}(\tau)\}}{\mathcal{F}\{\phi_{\rho\rho}(\tau)\}} \tag{5.122}$$

where the transforms

$$\begin{aligned}\mathcal{F}\{\phi_{\rho P}(\tau)\} &\equiv \int_{-\infty}^{\infty} e^{i\omega\tau}\phi_{\rho P}(\tau)d\tau \\ \mathcal{F}\{\phi_{\rho\rho}(\tau)\} &\equiv \int_{-\infty}^{\infty} e^{i\omega\tau}\phi_{\rho\rho}(\tau)d\tau\end{aligned} \tag{5.123}$$

are known as the *cross spectral density* and the *input* or *reactivity spectral density*, respectively.

If the control rod (or other neutron absorber) position is varied randomly over a narrow range and a neutron detector response is recorded, the reactivity autocorrelation function, $\phi_{\rho\rho}$, and the reactivity-power cross-correlation function, $\phi_{\rho P}$, can be constructed by numerically evaluating the defining integrals over a period of about 5 min using a series of delay intervals, τ, increasing in discrete steps of about $\Delta\tau = 0.01$ s. The cross spectral density and reactivity spectral density can then be calculated by numerically evaluating the defining Fourier transform; for example,

$$\mathcal{F}\{\phi_{\rho P}(\tau)\} \simeq \sum_{n} \phi_{\rho P}(n\Delta\tau)(\cos n\omega\Delta\tau + i\sin n\omega\Delta\tau)\Delta\tau \tag{5.124}$$

where n varies from a large negative integer to a large positive integer. There are sophisticated fast Fourier transform methods which are used in practice for evaluation of the cross and reactivity spectral densities.

Experimentally, it is convenient to use a reactivity variation that changes from positive to negative at definite times, so that the reactivity autocorrelation function is nearly a delta function. For such a pseudorandom binary reactivity variation,

$$\phi_{\rho\rho}(\tau - t') \simeq \text{const}\,\delta(t - t') \tag{5.125}$$

In this case, it follows from Eq. (5.121) that

$$\begin{aligned} &\phi_{\rho P}(\tau) \simeq \text{const}\, h(\tau) \\ &\mathcal{F}\{\phi_{\rho P}(\tau)\} \simeq \text{const}\, H(-i\omega) \end{aligned} \tag{5.126}$$

and that the amplitude and phase of the transfer function can be extracted from the computation of only the cross correlation function. By repeating the Fourier transforms of Eq. (5.123) for different values of ω, the frequency dependence of $H(-i\omega)$ can be determined.

Reactor Noise Method

Minor and essentially random variations in temperature and density within a nuclear reactor, such as bubble formation in boiling water reactors, produce small and essentially random reactivity variations. Autocorrelation of the response of a neutron detector, which is proportional to the reactor neutron population or power, provides a means of determining the amplitude of the reactor transfer function from this noise. Writing the power autocorrelation function

$$\phi_{PP}(\tau) \equiv \frac{1}{2T}\int_{-T}^{T} P_1(t) P_1(t+\tau)\,dt \tag{5.127}$$

and using Eq. (5.119) yields

$$\begin{aligned} \phi_{PP}(\tau) &= \frac{1}{2T}\int_{-T}^{T} dt \int_0^\infty h(t')\rho_{\text{ex}}(t-t')dt' \int_0^\infty h(t'')\rho_{\text{ex}}(t+\tau-t'')dt'' \\ &= \int_0^\infty h(t') \int_0^\infty h(t'')\left[\frac{1}{2T}\int_{-T}^{T} \rho_{\text{ex}}(t-t')\rho_{\text{ex}}(t+\tau-t'')dt\right]dt'dt'' \\ &= \int_0^\infty h(t')dt' \int_0^\infty h(t'')\left[\phi_{\rho\rho}(\tau+t'-t'')\right]dt'' \end{aligned} \tag{5.128}$$

Fourier transformation then gives

$$H(-i\omega)H(i\omega) = |H(i\omega)|^2 = \frac{\mathcal{F}\{\phi_{PP}(\tau)\}}{\mathcal{F}\{\phi_{\rho\rho}(\tau)\}} \simeq \frac{\mathcal{F}\{\phi_{PP}(\tau)\}}{\text{const}} \tag{5.129}$$

where the fact that the autocorrelation function of a random reactivity input is a delta function, the Fourier transform of which is a constant, has been used in writing the final form. Thus the amplitude, but not the phase, of the reactor transfer function can be determined from autocorrelation of the reactor noise. Again, the frequency dependence is determined by taking the Fourier transform with respect to various frequencies, ω. This provides a powerful technique for online, nonintrusive monitoring of an operating reactor for component malfunction and incipient problems.

Example 5.9: Reactor Transfer Function Measurement in EBR-I. The reactor transfer function measurement on the early EBR-I sodium-cooled, metal fuel fast reactor provides a good example of the physical insight provided by transfer function measurements. The Mark II core was stable at lower power levels, but at moderate power levels an oscillatory power was observed. The measured transfer function is shown in Fig. 5.6: in part (a) for several values of the coolant flow rate (gallons

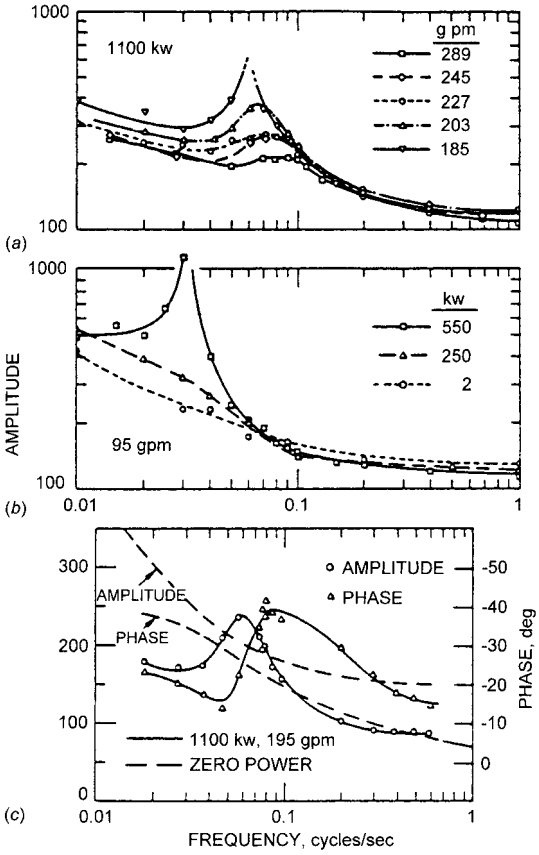

Fig. 5.6 Reactor transfer function EBR-1: (a) as a function of coolant flow rate; (b, c) as a function of reactor power. (From Ref. 9; used with permission of American Nuclear Society.)

per minute), and in parts (*b*) and (*c*) for several values of the reactor power level. At the lower coolant flow rates and the higher power levels there is a pronounced resonance in the transfer function, suggesting an incipient instability, which is not present at the higher flow rates and lower power levels.

The Mark II core was known to have a prompt reactivity feedback which added reactivity with an increase in power or a decrease in coolant flow. However, when steady state was achieved following an increase in power at constant flow, the net change in reactivity was negative, indicating an overall asymptotic power coefficient that was negative. Calculations indicated that the Doppler effect was negligible, that bowing of the fuel rods toward the center of the core contributed significant positive reactivity, and that the outward expansion of the structural plates supporting the fuel rods led to a delayed outward movement of the fuel rods that contributed negative reactivity.

A three-temperature model was used to explain the phenomena observed. The fast positive reactivity was modeled as due to the fuel bowing, and the delayed negative reactivity was modeled as the fuel motion due to the delayed outward motion of the fuel rods upon expansion of the structural plates. Heat conduction plus convection for the two separate structural effects led to a three-term representation of the power feedback. After correcting for the frequency dependence of the oscillatory heat flow, the model achieved very good agreement with the transfer function measurements.

5.11
Reactor Transients with Feedback

The dynamics equations are intrinsically nonlinear when feedback effects are included. The calculation of reactor transients is carried out with very sophisticated computer codes which model in detail the coupled dynamics of the neutrons, temperature, flow, structural motion, change of state, and so on. However, some physical insight as to the effects of feedback can be obtained by considering the simple model of Section 5.4 in the presence of feedback.

The point kinetics equations with feedback may be written in the one delayed neutron group approximation as

$$\begin{aligned} \frac{dn(t)}{dt} &= \left(\frac{\rho_{\text{ex}} + \alpha_F T(t) - \beta}{\Lambda} \right) n(t) + \lambda C(t) \\ \frac{dC(t)}{dt} &= \frac{\beta}{\Lambda} n(t) - \lambda C(t) \end{aligned} \tag{5.130}$$

where a feedback reactivity $\rho_f(t) = \alpha_f T(t)$ has been added to the step reactivity insertion ρ_{ex}. We will treat the temperature, T, as either a fuel temperature or a lumped fuel–moderator temperature which satisfies

$$\rho C_P \frac{dT(t)}{dt} = E_f \Sigma_f \, \text{v} n(t) - \theta T(t) \tag{5.131}$$

where ρ is the density, E_f the deposited energy per fission, and $\theta \approx \kappa/(\text{heat transfer distance})$ account for conductive heat removal. In Section 5.4 we found that the response to a step subprompt-critical ($\rho_{ex} < \beta$) reactivity insertion into a critical reactor was a prompt jump that changed the neutron density from n_0 to $n_0/(1 - \rho_{ex}/\beta)$ in a time on the order of the neutron generation time, Λ, followed by a slow rise ($\rho_{ex} > 0$) or decay ($\rho_{ex} < 0$) of the neutron density on the delayed neutron decay constant time scale. We examine these two phases of the transient separately in the presence of feedback.

Step Reactivity Insertion ($\rho_{ex} < \beta$): Prompt Jump

During the initial phase of the transient for a few Λ following the reactivity insertion, the delayed neutron precursor decay source is constant at the critical equilibrium value $\lambda C_0 = (\beta/\Lambda)n_0$. In the absence of feedback, the solution of Eq. (5.130) in this case is

$$n(t) = n_0 \exp\left(\frac{\rho_{ex} - \beta}{\Lambda} t\right)\left[1 + \frac{\beta}{\Lambda}\int_0^t \exp\left(-\frac{\rho_{ex} - \beta}{\Lambda} t'\right) dt'\right] \simeq \frac{n_0}{1 - \rho_{ex}/\beta} \tag{5.132}$$

Assuming that the feedback is on the fuel temperature, which responds instantaneously to an increase in the fission rate, the corresponding solution with feedback reactivity is

$$n(t) = n_0 \exp\left(\frac{\rho_{ex} + \alpha_f T(t) - \beta}{\Lambda} t\right) \times \left[1 + \frac{\beta}{\Lambda}\int_0^t \exp\left(-\frac{\rho_{ex} + \alpha_f T(t') - \beta}{\Lambda} t'\right) dt'\right] \tag{5.133}$$

On this short time scale $t \sim \Lambda \ll \rho C_p/\theta$, the solution of Eq. (5.131) is

$$T(t) \simeq \frac{E_f \nu \Sigma_f}{\rho C_p}\int_0^t n(t')dt' \tag{5.134}$$

If the feedback is negative ($\alpha_f < 0$), the effect of the feedback is to reduce the magnitude of the input reactivity step. If $\rho_{ex} > 0$, n and T increase in time and $\rho_f = \alpha_f T < 0$; if $\rho_{ex} < 0$, n and T decrease in time and $\rho_f = \alpha_f T > 0$; ($T_0 = 0$). If the feedback is positive ($\alpha_f > 0$), the effect of the feedback is to enhance the magnitude of the input reactivity step. If $\rho_{ex} > 0$, n and T increase in time and $\rho_f = \alpha_f T > 0$; if $\rho_{ex} < 0$, n and T decrease in time and $\rho_f = \alpha_f T < 0$. Thus negative feedback reactivity would reduce the magnitude of the prompt jump and perhaps reverse the sign if the feedback reactivity exceeds the input reactivity; positive feedback reactivity would enhance the magnitude of the prompt jump.

Step Reactivity Insertion ($\rho_{ex} < \beta$): Post-Prompt-Jump Transient

We saw in Section 5.4 that in the absence of feedback, after the initial prompt jump in the neutron density on the prompt neutron time scale, the subsequent transient evolves on the slower time scale of the delayed neutron precursor decay:

$$n(t) = \frac{n_0 \exp\{(\lambda\rho_{ex}/\beta)t/(1-\rho_{ex}/\beta)\}}{1-\rho_{ex}/\beta} \tag{5.135}$$

For the problem with feedback, we make use of the prompt-jump approximation (set $dn/dt = 0$) and solve Eqs. (5.130) to obtain

$$n(t) \simeq \frac{n_0 \exp\left\{-\lambda\left(t - \int_0^t \frac{dt'}{1-[\rho_{ex}+\alpha_f T(t')]/\beta}\right)\right\}}{1-[\rho_{ex}+\alpha_f T(t)]/\beta} \tag{5.136}$$

which reduces to Eq. (5.135) when $\alpha_f = 0$. Note that Eq. (5.136) is valid only for the time after the prompt jump in neutron density between $t = 0$ and $t = t_{pj} \approx \Lambda$. This equation evaluated at t_{pj} implies an effective prompt jump from $n_0 \to n_0/[1 - (\rho_{ex} + \alpha_f T(t_{pj}))/\beta]$, to be compared with the effective prompt jump from $n_0 \to n_0/(1-\rho_{ex}/\beta)$ in the case without feedback implied by Eq. (5.135). Equation (5.131) can be solved formally for the temperature

$$T(t) = \frac{E_f \nu\Sigma_f}{\rho C_p} \int_0^t n(t') \exp -(\theta/\rho C_p)(t-t')dt' \tag{5.137}$$

The presence of feedback can have a dramatic effect on the course of the transient. Consider a positive step reactivity insertion, $0 < \rho_{ex} < \beta$, which without feedback would result in an exponentially increasing neutron density with period $(\beta/\rho_{ex} - 1)/\lambda$. With negative reactivity feedback ($\alpha_f < 0$), the period becomes longer (the rate of increase is slower), or even becomes negative (the neutron density decreases in time) if $|\alpha_f|T(t)$ becomes greater than ρ_{ex}. For a negative step reactivity insertion, $\rho_{ex} < 0$, and negative reactivity feedback, the presence of feedback with the decreasing temperature causes the decay in the neutron density to become slower and even reverse and start increasing if $|\alpha_f T(t)|$ becomes greater than $|\rho_{ex}|$. Thus a reactor with a negative temperature coefficient of reactivity will adjust automatically to a step reactivity insertion by seeking a new critical condition. For example, when a cold reactor is started up by withdrawing the control rods to produce an increasing neutron population and increasing fission heating, the negative reactivity will increase also, until the reactor reaches a new temperature and neutron population at which it is just critical. A negative temperature coefficient of reactivity also allows a reactor to automatically *load follow* (an increase in power output demand will result in a decrease in coolant inlet temperature, which produces a positive reactivity that causes the neutron population and the fission rate to increase until a new critical condition is reached at higher power).

5.12
Reactor Fast Excursions

The examination of hypothetical accidents requires the analysis of fast, supercritical excursions in the neutron population in a reactor. Although this analysis is done with sophisticated computer codes, which solve the coupled neutron–thermodynamics–hydrodynamics equation of state equations, there are several analytical models which provide physical insight into the phenomena of fast supercritical reactor excursions. Delayed neutron precursors respond too slowly to be important in such transients and may be neglected.

Step Reactivity Input: Feedback Proportional to Fission Energy

The prompt neutron kinetics equation for a step reactivity input $\Delta k_0 > k\beta$ and a feedback negative reactivity proportional to the cumulative fission energy release is described by

$$\frac{1}{P}\frac{dP(t)}{dt} = \frac{k-1}{\Lambda} = \frac{\Delta k_0 - \alpha_E E(t)}{\Lambda} = \frac{\Delta k_0}{\Lambda} - \frac{\alpha_E}{\Lambda}\int_0^t P(t')dt' \tag{5.138}$$

where Δk_0 is measured relative to prompt critical and

$$E(t) \equiv \int_0^t P(t')dt', \qquad \alpha_E \equiv \frac{\partial k}{\partial E} \tag{5.139}$$

The solution of Eq. (5.139) is

$$E(t) = \frac{(\Delta k_0/\Lambda) + R}{\alpha E/\Lambda}\frac{1 - e^{-Rt}}{\frac{[(R+\Delta k_0/\Lambda)]}{[(R-\Delta k_0/\Lambda)]}e^{-Rt} + 1} \tag{5.140}$$

where

$$R \equiv \sqrt{\left(\frac{\Delta k_0}{\Lambda}\right)^2 + 2\left(\frac{\alpha_E}{\Lambda}\right)P_0} \tag{5.141}$$

For transients initiated from low initial power level, P_0, $R \approx \Delta k_0/\Lambda$ and

$$E(t) \simeq \left(2(\Delta k_0/\alpha_E)(1 - e^{-(\Delta k_0/\Lambda)t})\right) \Big/ \left(\frac{2(\Delta k_0/\Lambda)^2}{(\alpha_E/\Lambda)P_0}e^{-(\Delta k_0/\Lambda)t} + 1\right) \tag{5.142}$$

The instantaneous power is

$$\begin{aligned} P(t) = \dot{E}(t) &= \frac{2R^2}{\alpha_E/\Lambda}\left(\frac{R + (\Delta k_0/\Lambda)}{R - (\Delta k_0/\Lambda)}\right)e^{-Rt} \Big/ \left(\left(\frac{R + (\Delta k_0/\Lambda)}{R - (\Delta k_0/\Lambda)}\right)e^{-Rt} + 1\right)^2 \\ &\simeq \frac{4(\Delta k_0/\Lambda)^4}{(\alpha_E/\Lambda)^2 P_0}e^{-(\Delta k_0/\Lambda)t} \Big/ \left[2\frac{(\Delta k_0/\Lambda)^2}{(\alpha_E/\Lambda)P_0}e^{-(\Delta k_0/\Lambda)t} + 1\right]^2 \end{aligned} \tag{5.143}$$

where the second form is valid only for low initial power.

Equation (5.143) describes a symmetrical power excursion that increases to a maximum power $P_{\max} = (\Delta k_0/\Lambda)^2/2(\alpha_E/\Lambda)$ at $t \approx 1.3/(\Delta k_0/\Lambda)$ and then decreases to zero. The width of the power burst at half maximum is $\approx 3.52/(\Delta k_0/\Lambda)$, and the total fission energy produced in the burst is $2\Delta k_0/\alpha_E$.

Ramp Reactivity Input: Feedback Proportional to Fission Energy

If, instead of a step reactivity input, the external reactivity input is a ramp (e.g., as might occur in rod withdrawal), Eq. (5.138) becomes

$$\frac{1}{P}\frac{dP(t)}{dt} = \frac{at - \alpha_E E(t)}{\Lambda} = \frac{at}{\Lambda} - \frac{\alpha_E}{\Lambda}\int_0^t P(t')dt' \tag{5.144}$$

which has a solution of the form

$$E(t) = \frac{a}{\alpha_E}t + \text{periodic function} \tag{5.145}$$

The power level has a background (a/α_E) upon which is superimposed a series of oscillations as the net external plus feedback reactivity oscillates about prompt critical ($\rho = \beta$). We now examine one of the power oscillations. Differentiating Eq. (5.144) yields an equation for the instantaneous period $\theta \equiv (dP/dt)/P$:

$$\frac{d\theta(t)}{dt} = \frac{a}{\Lambda} - \frac{\alpha_E}{\Lambda}P(t) \tag{5.146}$$

which may be combined with Eq. (5.144) to obtain

$$\frac{dP}{d\theta} = \frac{\theta P}{a/\Lambda - (\alpha_E/\Lambda)P} \tag{5.147}$$

This equation has the solution

$$\frac{1}{2}\theta^2(t) = \frac{a}{\Lambda}\ln\frac{P(t)}{P_0} - \frac{\alpha_E}{\Lambda}[P(t) - P_0] \tag{5.148}$$

The maximum power at the peak of the oscillation occurs when $\theta = 0$ and thus satisfies

$$P_{\max} = P_0 + \frac{a}{\alpha_E}\ln\frac{P_{\max}}{P_0} \simeq \frac{a}{\alpha_E}\ln\frac{P_{\max}}{P_0} \tag{5.149}$$

where the second form is only valid for $P_0 \ll P_{\max}$, where $P_0 = a/\alpha_E$ now refers to the background power at the beginning of the oscillation.

Step Reactivity Input: Nonlinear Feedback Proportional to Cumulative Energy Release

The Doppler feedback coefficient in large fast power reactors is not constant but is calculated to vary approximately inversely with fuel temperature, and theoretical considerations suggest that it varies inversely with fuel temperature to the $\frac{3}{2}$ power.

If we assume no heat loss from the fuel and constant specific heat to relate the fuel temperature increase during a transient to the cumulative fission energy release, we can represent a broad class of temperature-dependent feedback reactivities as $\alpha_E E^n$, where α_E now refers to the value of the feedback coefficient at the temperature at which the transient is initiated. In this case, the prompt neutron dynamics equation for a step external reactivity input Δk_0 is

$$\frac{1}{P}\frac{dP(t)}{dt} = \frac{\Delta k_0}{\Lambda} - \frac{\alpha'_E}{\Lambda}[E(t)]^n \tag{5.150}$$

This equation has the solution for the cumulative fission energy release

$$E(t) = \left[(n+1)\frac{\Delta k_0}{\alpha'_E}\right]^{1/n} \Big/ \left[1 + ne^{-(n\Delta k_0/\Lambda)t}\right]^{1/n} \tag{5.151}$$

which can be differentiated to obtain the instantaneous power

$$\begin{aligned} P(t) &= \dot{E}(t) \\ &= \left[(n+1)\frac{\Delta k_0}{\alpha'_E}\right]^{1/n} \left(n^2\frac{\Delta k_0}{\Lambda}\right) e^{-(n\Delta k_0/\Lambda)t} \Big/ \left[1 + ne^{-(n\Delta k_0/\Lambda)t}\right]^{1/(n+1)} \end{aligned} \tag{5.152}$$

Once again, the power increases to a maximum value, in this case

$$P_{\max} = \frac{n}{1+n}\left[\frac{(\Delta k_0/\Lambda)^{n+1}}{\alpha'_E/\Lambda}\right]^{1/n}$$

and then decreases to zero. The total energy release in the burst is $E_{\text{tot}} = [(1+n)\Delta k_0/\alpha'_E]^{1/n}$.

Bethe–Tait Model

It is clear that the course of a reactor excursion produced by a given external reactivity insertion is very sensitive to the feedback reactivity, hence to the evolution of the thermodynamic, hydrodynamic, and geometric condition of the reactor. The coupled evolution of these variables is calculated numerically in modern analyses. However, we can gain valuable physical insight by considering an early semianalytical model developed for fast metal fuel reactors. The prompt neutron dynamics are determined by

$$\begin{aligned} \frac{1}{P}\frac{dP(t)}{dt} &= \frac{k-1-\beta}{\Lambda} = \frac{\Delta k}{\Lambda} \\ &= \Delta k_0 + \Delta k_{\text{input}}(t) + \Delta k_{\text{displ}}(t) + \Delta k_{\text{other}}(t) \end{aligned} \tag{5.153}$$

where Δk_0 is the initiating step reactivity (relative to prompt critical), Δk_{input} is any control rod input, Δk_{displ} is the reactivity associated with a displacement of

core material due to pressure buildup, and Δk_{other} includes the Doppler effect and other nonhydrodynamic reactivity changes.

The displacement reactivity is given by

$$\Delta k_{\text{displ}}(t) = \int \rho(r,t)\mathbf{u}(r,t) \cdot \nabla w^{+}(r) dr \tag{5.154}$$

Here ρ is the material density, $\mathbf{u}(r,t)$ represents a material displacement from r to $r + \Delta r$, and $w^{+}(r,t)$ is the importance of a unit mass of material at location r to producing subsequent fission events. (The importance function is discussed in Chapter 13.)

The displacement is related to the pressure by the hydrodynamic equations

$$\rho \frac{\partial^2 \mathbf{u}(r,t)}{\partial t^2} = -\nabla p(r,t) \tag{5.155}$$

and

$$\frac{\partial \rho(r,t)}{\partial t} + \nabla \cdot \left[\rho(r,t) \frac{\partial \mathbf{u}(r,t)}{\partial t} \right] = 0 \tag{5.156}$$

An equation of state, represented symbolically as

$$p(r,t) = p(e(r,t), \rho(r,t)) \tag{5.157}$$

relates the pressure to the energy density, $e(r,t)$, and to the density. We neglect changes in density and work done in expansion or compression. Differentiating Eq. (5.154) twice and using Eq. (5.155) yields

$$\frac{\partial^2 \Delta k_{\text{displ}}}{\partial t^2} = -\int \nabla p(r,t) \cdot \nabla w^{+}(r) dr \tag{5.158}$$

The analysis proceeds by postulating that there is no feedback, except the Doppler effect, until the total energy generated in the core reaches a threshold value, E^*, at which point the core material begins to vaporize, thereby building up pressure, which causes the core to expand until the negative reactivity associated with expansion eventually terminates the excursion. Rather than carry through the rather involved derivation (see Ref. 9), we summarize the main results for a spherical core. When the energy, E, exceeds the threshold value, it subsequently increases as

$$E - E^* = E^* \left(e^{(\Delta k/\Lambda)(t - t^*)} - 1 \right) \tag{5.159}$$

The pressure near the center of the core is proportional to $E - E^* \approx E$, so that once it becomes large the pressure varies as

$$p \sim E N e^{(\Delta k/\Lambda)t} \tag{5.160}$$

The pressure gradient that tends to blow the core apart is proportional to p/R. Thus the radial acceleration produced by the pressure gradient goes as

$$\ddot{R} \sim |\nabla p| = \frac{C_1}{R} e^{(\Delta k/\Lambda)t} \tag{5.161}$$

Integrating this expression twice yields an expression for the instantaneous core radius

$$R'(t) \simeq R\left[1 + \frac{C_1 \Lambda^2}{(\Delta k)^2 R^2} e^{(\Delta k/\Lambda)t}\right] \tag{5.162}$$

The excursion terminates when the expansion increases the negative reactivity sufficiently to offset the initiating reactivity less any negative Doppler or rod input reactivity:

$$\Delta k_{\text{displ}}\left(R' - R\right) = \Delta k_0 - \Delta k_{\text{other}} - \Delta k_{\text{input}} = \Delta k' \tag{5.163}$$

which occurs at time t given by

$$e^{(\Delta k'/\Lambda)t} = \frac{(\Delta k')^3 R^2}{C_1 \Delta k_{\text{displ}} \Lambda^2} \tag{5.164}$$

The energy generated up to the time of termination is

$$E \sim \frac{(\Delta k')^3 R^2}{\Lambda^2} \tag{5.165}$$

Numerical calculations indicate that the approximate relationships above represent quite well excursions resulting from large initial reactivity insertions. For modest initiating reactivities, the expression

$$\left(\frac{E}{E^*} - 1\right) \sim \left[\frac{(\Delta k')^3 R^2}{\Lambda^2}\right]^{2/9} \tag{5.166}$$

is in better qualitative agreement with numerical results.

5.13 Numerical Methods

In practice, numerical methods are used to solve the neutron dynamics equations. The solution is made difficult by the difference in time scales involved. The prompt neutron time scale is on the order of $\Lambda = 10^{-4}$ to 10^{-5} s for thermal reactors or 10^{-6} to 10^{-7} s for fast reactors, while the delayed neutron time scales vary from tenths of seconds to tens of seconds. When ρ is significantly less than β, making the prompt jump approximation removes the prompt neutron time scale from the problem, and straightforward time-differencing schemes are satisfactory. When it

is necessary to retain the prompt neutron dynamics (i.e., for transients near or above prompt critical), the usual numerical methods for solving ordinary differential equations (e.g., Runge–Kutta) are limited by solution stability to extremely small time steps over which there is little change in the neutron population. However, a class of methods for solving stiff sets of ordinary differential equations (sets with very different time constants) have been developed (Refs. 2 and 7) and are now widely used for solution of the neutron dynamics equations.

References

1 D. Saphier, "Reactor Dynamics," in Y. Ronen, ed., *CRC Handbook of Nuclear Reactor Calculations II*, CRC Press, Boca Raton, FL (**1986**).

2 G. Hall and J. M. Watts, *Modern Numerical Methods for Ordinary Differential Equations*, Clarendon Press, Oxford (**1976**).

3 J. L. Duderstadt and L. J. Hamilton, *Nuclear Reactor Analysis*, Wiley, New York (**1976**), Chap. 6 and pp. 556–565.

4 A. F. Henry, *Nuclear-Reactor Analysis*, MIT Press, Cambridge, MA (**1975**), Chap. 7.

5 D. L. Hetrick, ed., *Dynamics of Nuclear Systems*, University of Arizona Press, Tucson, AZ (**1972**).

6 A. Z. Akcasu, G. S. Lellouche, and M. L. Shotkin, *Mathematical Methods in Nuclear Reactor Dynamics*, Academic Press, New York (**1971**).

7 C. W. Gear, *Numerical Initial Value Problems in Ordinary Differential Equations*, Prentice Hall, Englewood Cliffs, NJ (**1971**).

8 G. I. Bell and S. Glasstone, *Nuclear Reactor Theory*, Wiley (Van Nostrand Reinhold), New York (**1970**), Chap. 9.

9 H. H. Hummel and D. Okrent, *Reactivity Coefficients in Large Fast Power Reactors*, American Nuclear Society, La Grange Park, IL (**1970**).

10 L. E. Weaver, *Reactor Dynamics and Control*, Elsevier, New York (**1968**).

11 H. P. Flatt, "Reactor Kinetics Calculations," in H. Greenspan, C. N. Kelber, and D. Okrent, eds., *Computational Methods in Reactor Physics*, Gordon and Breach, New York (**1968**).

12 D. L. Hetrick and L. E. Weaver, eds., *Neutron Dynamics and Control*, USAEC-CONF-650413, U.S. Atomic Energy Commission, Washington, DC (**1966**).

13 M. Ash, *Nuclear Reactor Kinetics*, McGraw-Hill, New York (**1965**).

14 G. R. Keepin, *Physics of Nuclear Kinetics*, Addison-Wesley, Reading, MA (**1965**).

15 A. Radkowsky, ed., *Naval Reactors Physics Handbook*, U.S. Atomic Energy Commission, Washington, DC (**1964**), Chap. 5.

16 T. J. Thompson and J. G. Beckerly, eds., *The Technology of Nuclear Reactor Safety*, MIT Press, Cambridge, MA (**1964**).

17 L. E. Weaver, ed., *Reactor Kinetics and Control*, USAEC-TID-7662, U.S. Atomic Energy Commission, Washington, DC (**1964**).

18 J. A. Thie, *Reactor Noise*, Rowman & Littlefield, Totowa, NJ (**1963**).

19 J. Lasalle and S. Lefschetz, *Stability by Liapunov's Direct Methods and Applications*, Academic Press, New York (**1961**).

20 R. V. Meghreblian and D. K. Holmes, *Reactor Analysis*, McGraw-Hill, New York (**1960**), Chap. 9.

Problems

5.1. The absorption cross section in a bare, critical thermal reactor is decreased by 0.5% by removing a purely absorbing material. Calculate the associated reactivity.

5.2. A bare metal sphere of essentially pure ^{235}U is assembled, and the output of a neutron detector is observed, after an initial transient, to be increasing exponentially with a period $T = 1$ s. The neutron effectiveness values for the six delayed neutron groups are calculated to be $\gamma_i = 1.10, 1.03, 1.05, 1.03, 1.01$, and 1.01. What is the effective multiplication constant, k, for the assembly?

5.3 Using the one-delayed precursor group approximation, prompt-jump approximation, and the reactor parameters $\beta = 0.0075$, $\lambda = 0.08\ \text{s}^{-1}$, $\Lambda = 6 \times 10^{-5}$ s, solve for the time dependence of the neutron population over the interval $0 < t < 10$ s following the introduction of a ramp reactivity $\rho(t) = 0.1\beta t$ into a critical reactor for $0 < t < 5$ s. Such a reactivity insertion might result from partial withdrawal of a control rod bank.

5.4. A pulsed neutron measurement was performed in an assembly with $\beta = 0.0075$ and $\Lambda = 6 \times 10^{-5}$. An exponential prompt neutron decay constant $\alpha_0 = -100\ \text{s}^{-1}$ was measured. What are the reactivity and effective multiplication constant of the assembly?

5.5. A control rod was partially withdrawn from a critical nuclear reactor for 5 s, then reinserted to bring the reactor back to critical. The reactivity worth of the partial rod withdrawal was $\rho = 0.0025$. Use the prompt-jump approximation and a one delayed neutron group approximation to calculate the neutron and precursor populations, relative to the initial critical populations, for times $0 < t < 10$ s. Use the neutron kinetic parameters $\beta = 0.0075$, $\lambda = 0.08\ \text{s}^{-1}$, and $\Lambda = 6 \times 10^{-5}$ s.

5.6. A control rod bank is scrammed in an initially critical reactor. The signal of a neutron detector drops instantaneously to one-third of its prescram level, then decays exponentially. Assume one group of delayed neutrons with $\beta = 0.0075$ and $\lambda = 0.08$ s, and use $\Lambda = 10^{-4}$ s for the reactor lifetime. What is the reactivity worth of the control rod bank? How long is needed for the power level to reach 1% of the initial prescram level?

5.7. Plot the real and imaginary parts of the zero-power transfer function versus ω ($s = i\omega$) for a ^{235}U reactor using a one

delayed neutron group model with $\beta = 0.0075$, $\lambda = 0.08\ \text{s}^{-1}$, and $\Lambda = 6 \times 10^{-5}$ s.

5.8 Calculate the Doppler reactivity temperature coefficient for a UO_2-fueled, H_2O-cooled thermal reactor with long fuel rods 1 cm in diameter operating with a fuel temperature of 450 K. The moderator macroscopic scattering cross section per atom of ^{238}U is 100. Take the resonance integral at 300 K as $I = 10$ barns.

5.9. Derive an expression for the calculation of a void temperature coefficient of reactivity for a pressurized water reactor (i.e., the temperature coefficient associated with a small fraction of the moderator being replaced with void). Repeat the calculation for when the water contains 1000 ppm ^{10}B as a "chemical shim."

5.10. Calculate the nonleakage reactivity temperature coefficient for a bare cylindrical graphite reactor with height-to-diameter ratio $H/D = 1.0$, $k_\infty = 1.10$, migration area $M^2 = 400\ \text{cm}^2$, and moderator linear expansion coefficient $\theta_M = 1 \times 10^{-5}\ ^\circ\text{C}^{-1}$.

5.11. Calculate the reactivity defect in a PWR with fuel and moderator temperature coefficients of $\alpha_F = -1.0 \times 10^{-5}$ $\Delta k/k/^\circ\text{F}$ and $\alpha_M = -2.0 \times 10^{-4}$ $\Delta k/k/^\circ\text{F}$ when the reactor goes from hot zero power ($T_F = T_M = 530^\circ\text{F}$) to hot full power ($T_F = 1200^\circ\text{F}$ and $T_M = 572^\circ\text{F}$).

5.12. A critical reactor is operating at steady state when there is a step reactivity insertion $\rho = \Delta k/k = 0.0025$. Use one group of delayed neutrons, the parameters $\beta = 0.0075$, $\lambda = 0.08\ \text{s}^{-1}$, and $\Lambda = 6 \times 10^{-5}$ s, and a temperature coefficient of reactivity $\alpha_T = -2.5 \times 10^{-4}\ ^\circ\text{C}^{-1}$. Assume that the heat removal is proportional to the temperature. Write the coupled set of equations that describe the dynamics of the prompt and delayed neutrons and the temperature. Linearize and solve these equations (e.g., by Laplace transform).

5.13. Calculate the power threshold for linear stability (in units of $P_0 X_F/\beta$) from Eq. (5.111) for $X_F/X_M = -0.25$ and -0.50 and for $\omega_M = 0.1$, 0.25, and 0.5.

5.14. Analyze the linear stability of a one-temperature model for a nuclear reactor in which the heat is removed by conduction with time constant ω_R^{-1} and in which there is an overall negative steady-state power coefficient, $X_R < 0$. Is the reactor stable at all power levels?

5.15. Repeat problem 5.14 for convective heat removal.

5.16. Calculate and plot the power burst described by Eq. (5.143) for a fast reactor with generation time $\Lambda = 1 \times 10^{-6}$ s and negative energy feedback coefficient $\alpha_E = -0.5 \times 10^{-6}$

$\Delta k/k$/MJ into which a step reactivity insertion of $\Delta k_0 = +0.02$ takes place at $t = 0$. Use $P_0 = 100$ MW.

5.17. A control rod is partially withdrawn (assume instantaneously) from a ^{235}U-fueled nuclear reactor that is critical and at low power at room temperature. The signal measured by a neutron detector is observed to increase immediately to 125% of its value prior to rod withdrawal, and then to increase approximately exponentially. What is the reactivity worth of the control rod? What is the value of the exponent that governs the long-time exponential increase of the signal measured by the neutron detector?

5.18. In a cold critical PWR fueled with 4% enriched UO_2, the control rod bank is withdrawn a fraction of a centimeter, introducing a positive reactivity of $\rho = 0.0005$. The neutron flux begins to increase, increasing the fission rate. Discuss the feedback reactivity effects that occur as a result of the increasing fission heating.

5.19. Use the temperature coefficients of reactivity given in Table 5.3 to calculate the change in reactivity when the core temperature in an oxide-fueled fast reactor increases from 300°C to 500°C. Assume uniform temperatures in fuel, coolant, and structure. Repeat the calculation for a fuel temperature increase to 800°C and a coolant and structure temperature increase to 350°C.

5.20.* Solve Eqs. (5.133) and (5.134) to calculate the response of the neutron population in a UO_2-fueled PWR to step rod withdrawal with reactivity worth $\rho = 0.002$, taking into account a negative fuel Doppler feedback coefficient of -2×10^{-6} $\Delta k/k$/K. The reactor has neutronics properties ($\beta = 0.0065$, $\lambda = 0.08$ s^{-1}, $\Lambda = 1.0 \times 10^{-4}$), fission heat deposition in the fuel $v n \Sigma_f E_f = 250$ W/cm^3, and fuel properties $\rho = 10.0$ g/cm^3 and $C_p = 220$ J/kg. (*Hint*: It is probably easiest to do this numerically.)

5.21. Evaluate the resonance escape probability moderator temperature coefficient of reactivity of Eq. (5.87) for a UO_2 reactor consisting of assemblies of 1-cm-diameter fuel pins of height H in a water lattice with $\Sigma_p/N_M = 100$ and fuel density $\rho = 10$ g/cm^3. Use $\theta_M = 1 \times 10^{-4}$/K for the linear coefficient of expansion for water.

5.22. Derive an explicit expression for the thermal utilization temperature coefficient of reactivity of Eq. (5.89) by using Eqs. (3.90) and (3.92) to evaluate the $\partial \Sigma_a^F / \partial \xi$ and $\partial \xi / \partial T_F$

* Problem 5.20 is a longer problem suitable for a take-home project.

terms and equivalent relations to evaluate the $d\Sigma_a^M/d\xi$ and $d\xi/dT_M$ terms.

5.23. In a "rod-drop" experiment, a control rod is dropped into a cold, critical reactor. The neutron flux is observed to immediately drop to one-half of its value prior to the rod drop and then decay slowly. Using a one-delayed-group model with delayed neutron fraction $\beta = 0.0065$ and decay constant $\lambda = 0.08/\text{s}$, determine the reactivity worth of the control rod.